Quantitative Analysis

2

Jeyne Pricylla Castro, Raquel Cardoso Machado, Daniel Fernandes Andrade, Diego Victor de Babos, Edenir Rodrigues Pereira-Filho, José Augusto Garcia, Marco Aurelio Sperança, Raimundo Rafael Gamela, and Vinícius Câmara Costa

2.1 Introduction

Over several decades, analytical chemistry has provided alternatives for the analysis of food, environmental samples, and technological materials, aiming at their elementary characterization [1]. The scientific literature in the area shows applications related to instrumental analytical techniques based on atomic absorption (AA) and emission (AE). Among the most widespread techniques for chemical sample analysis is inductively coupled plasma optical emission spectrometry (ICP-OES) [2]. ICP-OES requires the introduction of the sample typically in the form of a homogeneous liquid solution that must have some favorable characteristics for the

J. P. Castro · D. V. de Babos · E. R. Pereira-Filho (✉)
Group of Applied Instrumental Analysis, Department of Chemistry, Federal University of São Carlos, São Carlos, SP, Brazil
e-mail: erpf@ufscar.br

R. C. Machado
Embrapa Instrumentation, São Carlos, SP, Brazil

D. F. Andrade
Eurofarma, Rod. Presidente Castello Branco, Itapevi, SP, Brazil

J. A. Garcia
SG Soluções Científicas, São Carlos, SP, Brazil

M. A. Sperança
Group of Alternative Analytical Approaches (GAAA), Bioenergy Research Institute (IPBEN), Institute of Chemistry, São Paulo State University (UNESP), Araraquara, SP, Brazil

R. R. Gamela
Departamento de Engenharia de Processamento de Alimentos, Instituto Superior Politécnico de Gaza (ISPG), Gaza, Moçambique

V. C. Costa
Embrapa Instrumentação, São Carlos, SP, Brazil

G. Galbács (ed.), *Laser-Induced Breakdown Spectroscopy in Biological, Forensic and Materials Sciences*, https://doi.org/10.1007/978-3-031-14502-5_2

analysis, such as both low dissolved solids (typically less than 1%) and low acidity (in the order of 10% at most) [3].

The process of transforming a solid sample into a homogeneous aqueous solution is called acid digestion and can be carried out with the aid of concentrated or diluted acid mixtures [4]. The most used reagents are nitric (HNO_3) and hydrochloric (HCl) acids, as well as hydrogen peroxide (H_2O_2) combined with HNO_3. Digestion is complete after subjecting the sample and acid mixture to high temperatures and pressures [5]. The main goal is to make the constituent elements of the sample available in a dilute acid liquid medium, thus allowing their determination largely free from matrix interferences [3]. Furthermore, with the preparation of samples through acid digestion procedures, it becomes possible to carry out external calibration in the practical way of using aqueous solutions.

In several examples that employ solid samples (inorganic or organic), the requirements presented in the previous paragraph are met using simple procedures. Most food samples (meat, vegetables, fruits, flours, among others) and some environmental samples (sediment and soil) are examples of solid samples that can be converted in their entirety into liquid solutions after acid attack. The success of this conversion will depend on some parameters such as the sample mass and acid mixture ratio, time, and type of heating, such as conventional (convective) and assisted by microwave radiation [6]. However, some analytical matrices are extremely complex, recalcitrant or refractory, posing considerable challenges for the dissolution procedure. In many situations, it is necessary to use more oxidizing acids, such as sulfuric acid (H_2SO_4) and more aggressive reagents, such as hydrofluoric acid (HF) in the case of samples with high silicate contents [3]. In addition, sample preparation time can extend from a few minutes to several hours, compromising analytical throughput.

Thus, there is a need to propose analytical procedures that combine accessible techniques, high throughput, lower limits of detection, adequate values for accuracy, precision, and reduced cost *per* analysis. A viable alternative is the direct analysis of solid samples, such as using a laser [7]. This chapter is related to this theme and here we will try to approach the main characteristics related to the direct quantitative analysis of solid samples using laser-induced breakdown spectroscopy (LIBS) [8, 9].

LIBS is an analytical technique that emerged in the 1960s and became widespread from around 2000 onward, which can be applied for the direct analysis of samples of different nature, such as technological (glasses, alloys), radioactive, dangerous (explosives) and those with difficult access, such as soil of the planet Mars and direct analysis of deep waters. Most LIBS applications refer to the analysis of alloys [10], polymeric, agricultural, and geological materials [11]. These aspects will be addressed in the sections of this chapter and more attention was dedicated to solid samples. In the case of liquid and slurry samples, some examples are discussed by encapsulating the sample in a suitable substrate.

2.2 Description of the Main Matrix Effects in LIBS

In the last decades, the technological approaches that allowed direct solid samples analysis improved significantly. Nowadays, LIBS is one of the most used and reported technique in the scientific literature for this purpose [12]. However, besides advantages associated with LIBS technique, the analyst needs to deal with a huge challenge: matrix effects [9]. Actually, matrix effects are an analytical problem mainly associated to several analytical instrumental techniques, not exclusively, but mainly those that employ solid sample analysis. Several authors, such as Cremers and Radziemski [13] and Hahn and Omenetto [14], already discussed these topics. Radiziemski and Cremers [11] for instance, described several aspects that can compromise quantitative analysis: (1) microhomogeneity of the samples, (2) uniformity of the surface, (3) chemical matrix composition, and (4) physical matrix effects.

The chemical composition of the matrix is one of the most critical aspects of LIBS analysis because it influences the emission phenomenon of the analyte. Samples with organic composition (blood, biological tissues, biological microparticles) [15] or inorganic, as forensic samples such as explosive materials and soil fingerprinting, ceramic and nanomaterials [16] may lead to different and harmful matrix effects in the emission signal during the quantitative analysis [17]. The presence of easily ionizable elements (EIEs) in the sample matrix also can lead to chemical matrix effects due to changes in electronic density in the plasma, which shift the ionization equilibrium and compromise the accuracy of the results [18].

The physical properties of the sample are other important aspects that must be considered in LIBS analysis. Differences in these properties, such as humidity, heterogeneous particle size, thermal conductivity, absorption coefficient at the laser wavelength, sample temperature, heat of vaporization, uneven surface, pressure applied to sample to prepare pellets (if required), among others, may influence the amount of ablated mass, plasma formation and affect the vaporization, atomization and ionization processes [17–19].

The analysis of alloys was one of the first LIBS applications rapidly reported in the literature due to the sample characteristics. Sabsabi and Cielo [20] for instance, used LIBS for aluminum alloys quantitative analysis and determined Cu, Mg, Mn, and Si and employed external calibration. Afterward, Santos et al. [21] presented a review about the application of LIBS for macro- and micronutrient determination in leaves, roots, fruits, vegetables, wood, and pollen samples focusing on nutritional purposes. The authors discussed and compared univariate and multivariate calibration approaches. This comparison was also presented by Braga et al. [22] for metal determination in pellets of plants.

Matrix effects are evidence of the challenges in direct solid sample analysis by LIBS, mainly when the technique is used for quantitative analysis. An adjustment in experimental parameters, such as laser defocusing and changing the spectrometer

delay, may contribute to minimizing matrix effects, as was mentioned by Wang et al. [23]. However, some calibration strategies have stood out as a simple and efficient way to minimize or overcome matrix effects even in cases of complex samples [24].

Methods such as matrix-matching calibration (MMC), standard addition (SA), and internal standardization are mostly used when the goal of the analysis is the elemental determination. On the other hand, with intention of exploring other (and new) approaches, using different emission lines (and different sensitivities), reduced number of calibration samples compared to traditional calibration methods and employing physicochemical properties of laser-induced plasma species, novel calibration methods have been developed to minimizing matrix effects. The term calibration sample will be used in this and subsequent sections to describe samples that have known analyte concentration obtained by a reference or confirmatory method. It is important to mention that matrix effects will be never eliminated from an analytical chemistry method, and they are more intense in direct solid sample analysis. In addition, matrix effects can be also responsible for the lack of linearity in several LIBS applications. These methods are called non-traditional calibration strategies and will be discussed in the next sections [25].

Several authors highlight the importance of the matrix-matching approach in the calibration methods. In most cases, to ensure accurate and precise results in LIBS solid samples analysis, the physicochemical properties of the analyzed samples must be similar to samples used to build a calibration model, which is interesting because demonstrate the importance of considering the sample matrix to solve matrix effects [25].

It is a fundamental question in LIBS quantitative analysis, whether it is possible to obtain accurate analytical results without taking into account the differences in the matrix and the physicochemical properties of the calibration samples and the samples with unknown concentrations. A discussion of this question and potential answers are provided in this chapter.

2.3 Traditional Calibration Strategies Applied to LIBS

2.3.1 Matrix-Matching Calibration (MMC)

Calibration is still challenging for direct solid analysis [14, 26]. As discussed before, calibration in LIBS analysis is matrix dependent and limited by matrix effects originated from differences in the physical/chemical properties (i.e., density, porosity, moisture content, light absorption at the laser wavelength, surface roughness, etc.) among standards and samples. These dissimilarities can lead to different ablation behavior, hence resulting in an inadequate calibration that may provide biased results and compromise the accuracy, precision, and sensitivity of the analytical procedure [8, 27].

It is well known that calibration is an indispensable step in any quantitative analytical procedure [28]. Traditionally, calibration is based on recording a series of standards (calibration samples) to determine the correlation between the instrumental response and analyte concentration allowing to obtain the calibration function (usually linear) of which the analyte concentration at unknown samples is obtained [29]. External univariate calibration using matrix-matched standards is the most common approach in LIBS analysis. Ideally, the MMC aims an appropriate chemical and physical match between the calibration samples and the samples with unknown concentrations [25].

Alternatives to obtain appropriate calibration samples are certified reference materials (CRMs) and laboratory-prepared "home-made" standards by mixing samples or synthetic standards based on the main sample matrix component using similar materials (e.g., salts and oxides). The general preparation processes involve milling the sample material, spiking it with suitable elements, mixing to homogenization, diluting, drying if necessary, and pressing it into a pellet. The calibration samples are prepared in an adequate diluent such as cellulose powder [30, 31], salts [31–33], or original samples [34] as well as paraffin wax [35] and polyvinyl alcohol (PVA) [36, 37] for liquid matrices. Other materials have been explored, for example, Silvestre et al. [38] prepared synthetic standard materials by adding increasing concentrations of K and Mg in wood, filter paper, and babassu mesocarp for further plant sample analysis by LIBS. However, it is important to point out that preparing highly matrix-matched standards is a difficult task in practice. Nevertheless, CRMs are expensive, its availability is limited, and do not either cover the different types of matrices or range of concentrations. Despite that, MMC is a traditional calibration approach that works for a variety of samples, especially for simple matrix content. With respect to this, Table 2.1 shows some applications using the MMC procedure for different samples.

For instance, de Carvalho et al. [42] demonstrated the applicability of LIBS for the determination of elemental content in pharmaceutical tablets. Calibration samples were obtained by mixing different samples with known reference values at different ratios, diluting with cellulose powder, and the resulted mixtures were homogenized using a cryogenic mill. The homogenized products were pressed into pellets and analyzed by LIBS. The results obtained for Ca, Cu, Fe, Mg, Mn, P, and Zn by the proposed LIBS method were in concordance with those obtained by the reference method involving microwave-assisted acid digestion and ICP-OES analysis.

Babos et al. [31] developed a quantitative method for the determination of Ca and P in mineral supplements. For calibration purposes, two different strategies were assessed: (1) six reference materials with different concentrations of the elements, and; (2) six solid standards prepared by diluting a reference material of mineral supplement using Na_2CO_3. The proposed methods were compared with other univariate calibration strategies and the results validated using reference values (reference material or ICP-OES data). Promising results (trueness around 90%) were achieved using the MMC, but the matrix effects were even better reduced by combining MMC and internal standardization using a carbon spectral line.

Table 2.1 Studies describing procedures for preparing matrix-matched calibration standards and their analytical application

Research area	Element	Sample	Goal	MMC procedure	Reference
Raw material analysis	B	Synthetic materials prepared from pure reagents	Development of LIBS procedure for direct determination of B content	Synthetic standards prepared by the binary mixture of H_3BO_3 and $C_6H_{12}O_6{\cdot}H_2O$ in powder form	Zhu et al. [39]
Raw material analysis	Cl	Cement	Chorine determination in cement-bound materials used in concrete structures	Original samples of cement with increasing amount of NaCl	Millar et al. [32]
Raw material analysis	Li	Ore mineral	Qualitative and semi-quantitative analysis of mineral samples	CRMs and synthetic glass standards prepared with increasing quantities of Li_2O, Al_2O_3, SiO_2, Rb_2O, and Cs_2O	Sweetapple and Tassios [40]
Food analysis	Ca, K and Mg	Milk and solid dietary supplements	Direct determination of macronutrients in powdered milk and dietary supplements	Original milk samples, and; dilution of dietary supplements with cellulose powder	Augusto et al. [30]
Food analysis	Ca, K, Mg, and Na	Meat	Quantitative determination of nutrients content in bovine and chicken meat	Original samples diluted with cellulose or spiked with increasing amounts of Ca, K, Mg, and Na	Leme et al. [41]
Environmental analysis	Ca, Mg, K, P, Cu, Mn, and Zn	Sugar cane leaves	Determination of macro and micronutrients in plant materials	Original samples diluted using extracted material (i.e., original samples after acid extraction)	Gomes et al. [34]
Food analysis	Ca and P	Mineral supplements for cattle	Calibration strategies for Ca and P determination in mineral supplements for cattle	Reference materials (RMs) or diluted with Na_2CO_3	Babos et al. [31]
Environmental analysis	K and Mg	Plant samples	Direct measurement of K and Mg in plant samples	Synthetic standards prepared by the addition of increasing concentrations of K and Mg in wood, babassu mesocarp, and filter paper	Silvestre et al. [38]
Agricultural inputs analysis	P	Fertilizers	Determination of P in commercial fertilizers	CRMs diluted with combined reagent containing $(NH_2)_2CO$, $CaCO_3$, $CaSO_4$ and KCl	Vieira et al. [33]

Pharmaceutical	Ca, Cu, Fe, Mg, Mn, P and Zn	Pharmaceutical tablets	Determination of macro and micronutrients in multielement tablets	Original samples and mixtures of commercial tablets with cellulose powder at different ratios	de Carvalho et al. [42]
Technological	Al and Pb	Printed circuit boards (PCBs)	Determination of Al and Pb in electronic circuits using different calibration strategies	Original samples	Babos et al. [24]

Millar et al. [32] studied the determination of Cl content in cement-bound materials by LIBS. The calibration curve was prepared using the incremental addition of water and NaCl to Portland cement. For the validation, test samples were obtained by adding different chlorine sources, e.g. NaCl was substituted by KCl, LiCl, or $CaCl_2$. Both calibration samples and test samples were dried at 105 °C, ground to a maximum particle size of 0.09 mm and pressed into pellets prior to LIBS analysis. Good accuracy results were reported for most samples, by comparing LIBS results to those obtained from potentiometric titration after acid digesting the samples. However, chlorine concentrations were systematically overestimated for some samples which were attributed to matrix effects.

The feasibility of using the original samples set for MMC method was demonstrated by Babos et al. [24]. The authors aimed to determine Al and Pb in electronic waste samples comparing different calibrations strategies. For the MMC procedure, the calibration curves ranged from 3.1 to 55 g kg^{-1} for Al and from 0.7 to 11.6 g kg^{-1} for Pb using four waste printed circuit boards (PCBs) as solid standards. These solid samples were previously digested using a mixture of acids in order to obtain reference values using ICP-OES. In addition, the authors obtained more than 400 spectra for sample in order to minimize sample microheterogeneity. The proposed method was validated using reference concentrations (ICP-OES data). Trueness (accuracy) values in the range from 99 to 116%, and relative standard deviation (RSD) values $\leq$4% were obtained.

More recently, a new MMC approach has been proposed based on a data pre-processing method namely adaptive subset matching (ASM) [43]. ASM first establishes a set of calibration models using the similarity of sample matrix properties. Therefore, for an unknown sample, it assigns the most suitable calibration model corresponding to the matrix properties to predict the analyte concentration. This procedure is performed by comparing the errors of each model. The model that presents the lowest error is assigned to the sample. The authors assessed the performance of the method on 90 coal samples, including 41 CRMs and 49 commercial. In order to minimize calibration error, coal powders were air-dried and pressed into pellets before LIBS analysis. Two multivariate regression methods, multiple linear regression (MLR) and partial least squares (PLS) regression, were performed to evaluate the effectiveness of ASM. Both methods were improved in combination with ASM, which efficiently reduced chemical matrix effects and improved LIBS quantification performance.

2.3.2 Internal Standardization

Internal standardization (signal normalization by an internal standard) is widely used in spectroanalysis and in some cases it is considered a calibration strategy. Due to its wide application in LIBS, authors of this chapter provide a discussion about this approach. To enable the possibility of using certain elements as an internal standard (IS) in analytical emission spectroscopy, some requirements need to be fulfilled prior to analysis, such as the element cannot be present in the sample at a considerable

concentration and, the emission line from the element of interest and the IS candidate should be free of self-absorption and spectral interference. Then, the IS needs to be added to the test samples and calibration samples in a proper way. Another practical and useful possibility is to employ an element that is already present in the samples and standards at a high concentration (thus its concentration can be considered more or less constant), such as C (in the case of organics) or Fe (in the case of steel). In addition to this, the physical and chemical characteristics of the internal standard and analyte should also be similar (e.g., excitation or ionization energy) [44].

The main goal of this strategy is to track and minimize instrumental and plasma fluctuations, matrix effects by rationing the analyte signal to that of the IS. Basically, it uses the division of the peak intensity or area of the emission line related to the analyte by the peak intensity or area of a selected emission line related to the IS. The IS has to be added to (or present in) all calibration and unknown samples in the same concentration. The calibration is actually executed in the same way as in external calibration, but the signal ratio is considered to be the analytical signal.

Elements that are expected to be absent or, at least, their concentration would be lower than limits of detection (LOD) and quantification (LOQ) can be added as potential ISs, such as yttrium (Y) [45, 46], scandium (Sc) and bismuth (Bi) [45]. Since the concentration of the IS in the whole set of samples is to be kept at the same level, it is expected that the signal of it only changes due to variations that the analyst desires to minimize or eliminate. Regarding LIBS analysis, selecting an IS is even more difficult, being almost impossible to use any element properly as an IS [47]. Despite that, the use of IS elements is desirable in LIBS analysis because it does help to minimize signal fluctuations caused by matrix or instrumental effects. This type of normalization of the signal using an IS element was applied in several cases in LIBS analysis and in some cases elements that are naturally present in constant concentration in the samples are used as IS (for example, C).

Sperança et al. [45] assessed the possibility of using Y, Sc, and Bi as IS in the determination of Al, Cr, Fe, Mg, Mn, and Ni in Cuban nickeliferous minerals using LIBS. For this, 0.1 g of each element (Y, Sc, and Bi) were accurately weighted in a slurry made with the samples and water and, this mixture was encapsulated in PVA (polyvinyl alcohol), a water-soluble polymer. The authors concluded that Y was the best choice as IS in this study reached a low standard error of validation (SEV) for the elements assessed. In another study, Zn was assessed as IS in the evaluation of soft tissues where the laser-tissue interaction was investigated based on the Zn signal response as the authors optimize the system [48]. Another manner to use internal standardization strategy in LIBS analysis is the use of an inner element, naturally present in the samples [49] or added for another reason, such as C from polymer used for encapsulating the sample and cellulose powder to improve the cohesion in pellets formation [36]. This strategy is feasible when the constituent of the sample that may be used as IS has the same concentration in the whole set of samples, such as C in an organic matrix (e.g., fresh vegetables) [49]. Andrade et al. [36] determined essential and toxic elements in suspended fertilizers using LIBS. For this, the authors encapsulated the samples using PVA and tested C emission signal as

IS, in which a constant mass of PVA was added in each sample. In this study, several normalization modes [50] were assessed for five elements (Cu, K, Mg, Mn, and Zn) and, specifically for Mg and Mn, the normalization mode that had the best results was from the ratio of the peak area normalized by the C emission signal (r of 0.9801 and 0.9834, respectively).

2.3.3 Standard Addition

Solid samples that present a complex matrix can significantly influence the laser pulse-sample interaction and, consequently the analyte emission signal. Thus, it can be difficult to obtain a correlation between the concentration and the emission signal of the analyte in the set of calibration samples and, in the analyzed samples of unknown concentration. In the multiple standard addition (SA) calibration method, a calibration curve is obtained for each unknown sample. As the same sample matrix is present in all calibration samples, the magnitude of matrix effects will be the same [2, 25].

Solid calibration samples in the SA procedure are prepared by adding increasing concentrations of the analyte using a salt, oxide, CRM, or aqueous solutions containing the analyte, to a fixed amount of sample. Five spiked samples are typically prepared *per* sample. When the addition of the analyte to the solid sample is done using a solid standard (a salt, for example), it is necessary to add a blank (which can be a binder) to make the sample mass up to a fixed amount so that the sample dilution will be constant in all samples. Furthermore, an efficient homogenization step of the sample and added analyte is required using an appropriate mill, in order not to compromise the precision of measurements. When the addition of the analyte to the solid sample is made using aqueous solutions, the steps of homogenization and drying of each prepared standard for further analysis are also necessary [51, 52]. Figure 2.1 illustrates an analyte addition procedure in the used calibration samples and the obtained multiple SA calibration curve.

The SA calibration strategy has some limitations. A significant number of additions have to be prepared and analyzed *per* sample. In addition, an efficient sample homogenization step is also necessary, resulting in low analytical throughput and additional costs. This calibration strategy is employed in quantitative analysis using LIBS [25]. An important aspect is to verify that the analyte signal remains in the linear proportionality range (signal saturation is avoided), but the slope of the addition plot is also significant. However, several elemental determinations using the analysis of solid samples with complex matrix by LIBS are described in the literature using SA as a calibration strategy, with acceptable analytical performance parameters.

Soils are a good example of samples with a chemically complex matrix, due to the variability of their composition associated with their geographic distribution [53]. Thus, SA was evaluated for the determination of Pb in soils, with different procedures for addition and homogenization of the analyte being reported in the preparation of solid standards for calibration [51, 53]. Yi et al. [53], prepared soil

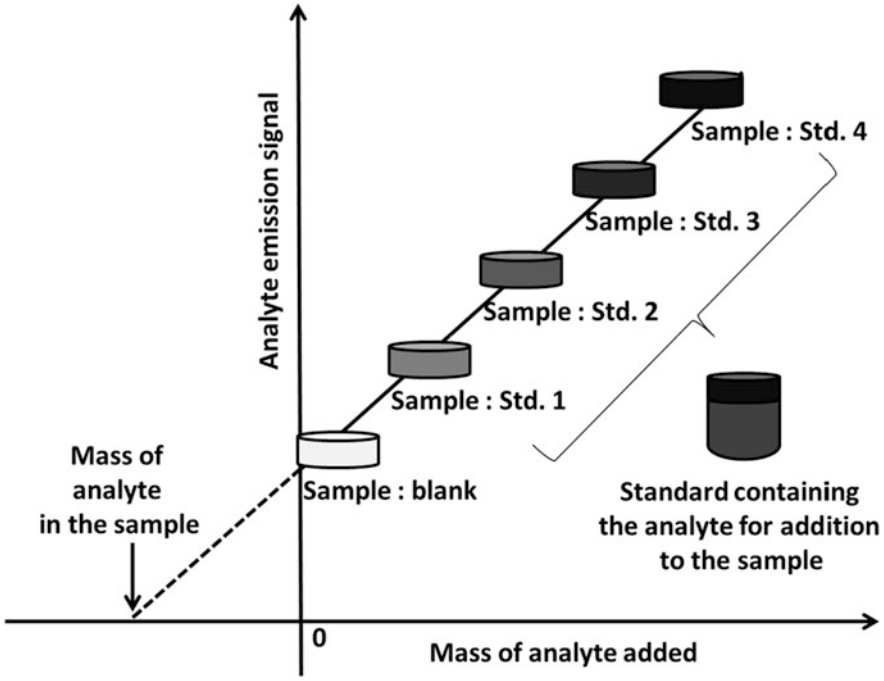

Fig. 2.1 Pictorial description of the SA procedure, which includes adding a standard (Std.) containing the analyte to the sample

suspensions containing aqueous $Pb(NO_3)_2$, which are homogenized using ultrasound, vacuum dried, ground in a mortar, and then pelleted for LIBS analysis. However, Wu et al. [51] added increasing concentrations of Pb using $Pb(NO_3)_2$ to the soil samples and then, diluted with soil samples collected at a depth of 3 m. Subsequently, they added water and homogenized the samples with a magnetic stirrer, dried and pressed them into pellets for further analysis. Note that the addition of the standard containing the analyte to the sample must be done carefully, so that it is homogeneously distributed in the sample and precision is not compromised.

Other analytes were also determined in solid samples by LIBS using SA calibration: (1) determination of Cu and Mn in the medicinal plant glycyrrhiza, using six solid calibration samples and Sr as internal standard [52]; (2) determination of Ca in coral skeleton, where nine calibration samples were used, six Ca I emission lines and, the intensity of a Sr II line were evaluated to normalize the intensity of the Ca I lines [54]; (3) quantitative analysis of *Mentha piperita* L. to determine Ba and Mn, using five calibration samples prepared by adding the analytes from an aqueous solution, and evaluating the precision and accuracy of metal determinations from the calibration curves obtained by the intensities of the emission lines of the analytes without normalization and normalized by the background, and by the lines of the Sr

internal standard, namely Sr I 460.73 nm (for Ba) and Sr II 407.77 nm (for Mn) [55]; among other examples.

Among the examples presented, it appears that several of them use the synergy between the SA and internal standardization calibration strategies to overcome the strong matrix effects and corrections of spectral fluctuations, using an appropriate internal standard [52, 54, 55].

The SA is a traditional calibration strategy that uses the sample itself for calibration adding the analyte to the sample at gradually increasing mass [56, 57]. However, besides of its advantages, this strategy requires a long time to prepare the calibration solid standard for each sample, which compromises the analytical frequency throughput. Therefore, it became not attractive and feasible for routine analysis, considering if an amount of sample needs to be analyzed.

This disadvantage led to the consideration of many other studies as an alternative to SA. One-point gravimetric standard addition (OPGSA) was proposed for matrix-matched standards to improve the LIBS analytical performance. For this strategy, only one calibration point is needed [31].

The linear model is calculated using two mixtures: (S1) sample plus blank (diluent) and, (S2) sample plus standard with known concentration of the analyte, e.g., certified reference material or salt. During the sample preparation, it is necessary that the sample:diluent and sample:standard ratios are the same, and a minor dilution factor can compromise the sensitivity for the determination of the analyte.

The concentration of the analyte in the sample employing this strategy is obtained by extrapolation of the calibration curve, as shown in Fig. 2.2. The x-axis corresponds to the mass of the analyte in the sample: 0 for S1 (sample + blank (diluent)) and, for S2 the mass of the added standard (known). On the y-axis is plotted the intensities of the selected emission line of the analyte for both pellets.

When the linear regression of both points is determined, the respective slope and linear coefficient (intercept) are used in Eq. 2.1 [31].

$$C_{\text{sample}} = \frac{|\ \text{Intercept}\ |}{\text{Slope}} \tag{2.1}$$

As only two calibration points are used, it is necessary to evaluate if the slope of the proposed method is statistically significant at a 95% of confidence level (p-value <0.05). This evaluation is performed comparing two variances: mean of squares of regression (MSR) and mean of squares of residue (MSr). These variances are compared through the F-test. The calculated F value (ratio between the variances described) is compared with the tabulated one, and it is required that the calculated should be at least 10-fold higher than the tabulated value (p value <0.05).

The proposed strategy is an efficient alternative to compensate matrix effects in solid analysis by LIBS and the data treatment is simpler than MEC (Multi-energy calibration, see next section), because only one emission line is used. However, the OPGSA sometimes presents limitations as the choice of an appropriate blank, and requires an efficient homogenization of the standards, which becomes the sample preparation for this strategy laborious [31, 58]. In addition, the linearity of the

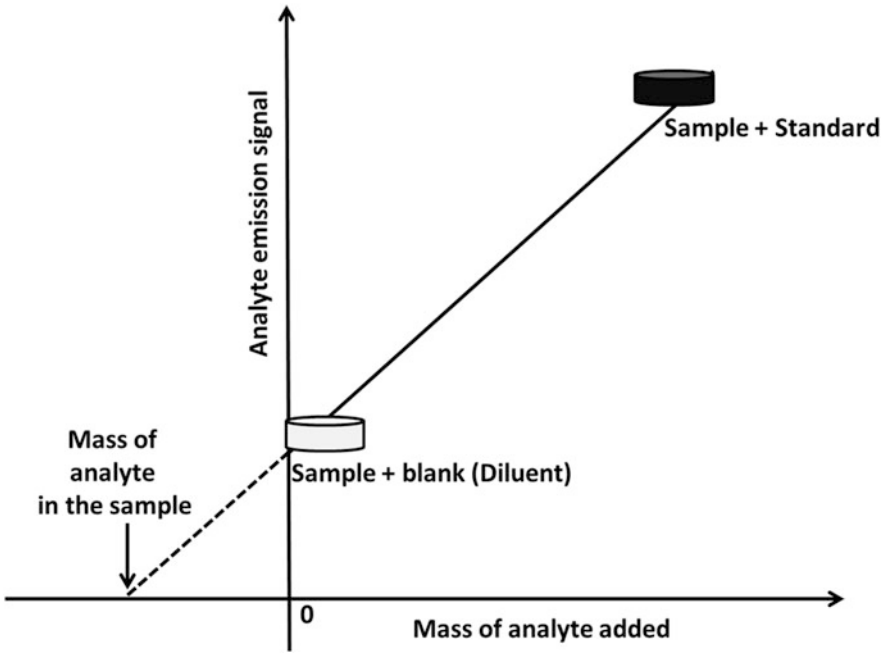

Fig. 2.2 Graphical description of the OP-GSA calibration strategy

proposed method must be checked, then the operator can verify first this condition using at least five calibration samples. This strategy can be useful for routine analysis, where the sample matrix is well known and presents low variability.

This strategy was applied for the determination of Ca and P in mineral supplements [31] and, for the determination of B, Fe, Dy, Gd, Nd, Pr, Sm, and Tb in electronic waste samples employing LIBS [58], showing the efficiency and its applicability to minimize matrix effects in complex samples.

2.4 Nontraditional Calibration Strategies

2.4.1 Multi-Energy Calibration

A LIBS spectrum is rich in information, and it can present several emission lines for a given analyte due to the various electronic transitions that occur between the fundamental and excited levels for a given element. So why not use all these analyte emission lines, with different sensitivities, to propose a calibration model for each analyzed sample? This is exactly what multi-energy calibration (MEC) proposes to obtain the calibration model: simultaneous use of several wavelengths of the analyte and only two calibration samples using the unknown sample itself.

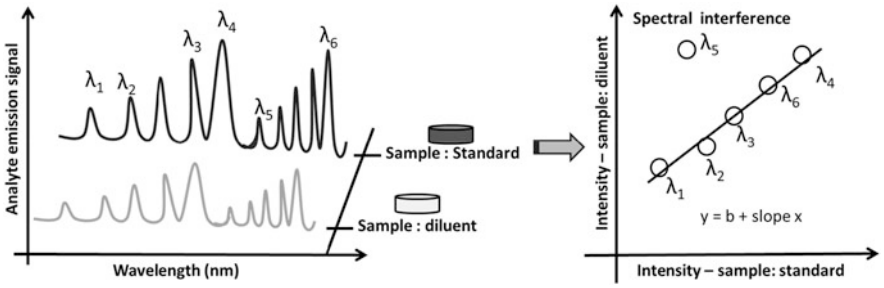

Fig. 2.3 Illustration of the LIBS emission spectra obtained from the analysis of the two calibration samples required *per* unknown sample and a linear MEC model highlighting an emission line (λ_5) with spectral interference

The MEC was initially proposed by Virgilio et al. [59], for elemental determination employing spectroanalytical techniques as ICP-OES, microwave-induced plasma optical emission spectrometry (MIP-OES), and high-resolution continuum source flame atomic absorption spectrometry (HR-CS-FAAS). In 2018, Babos et al. [60] reported the first study using MEC in the quantitative analysis of solid samples by LIBS.

Only two calibration samples *per* unknown sample are required to obtain the calibration model, which are prepared using: (1) one standard containing the analyte added to a given amount of sample and the other (2) a diluent (blank) added to the same amount of sample. The sample:standard and sample:diluent (w /w) ratio should be the same, and normally is 50:50 ratio (w /w). However, this proportion must be evaluated in some situations, so that it does not obtain a large dilution factor of the solid sample and does not compromise the monitoring of low sensitivity analyte emission lines. As the same amount of sample is present in the two calibration samples, a matrix-matching takes place [25, 59, 60].

The standard containing the analyte to be added in preparing the calibration samples can be a salt, oxide, CRM, or a sample with an analyte reference value, among others. The diluent (blank) can be a major constituent of the sample matrix, an appropriate binder or a sample that does not contain detectable analyte contents in its composition. As the addition of the standard and blank are made to solid samples, and in order to obtain precise and accurate measurements and not compromise the analytical parameters of the method, an efficient homogenization procedure must be performed before pelleting the two standards [25, 60].

In addition to obtaining an efficient matrix-matching, another advantage of using MEC is the possibility to identify analyte emission lines with spectral interference. In the MEC model, the interfered emission lines are identified as outliers (nonlinear trend). So it must be evaluated and removed from the linear model so that it does not compromise the accuracy of the analyte determination [25, 60]. Figure 2.3 illustrates the obtaining of the emission spectra of the two required calibration samples, and an MEC model with an emission line with spectral interference (outlier: emission line number 5, λ_5).

To obtain the linear MEC calibration model, the intensity values monitoring the different emission lines of the analyte in the standard prepared by adding a standard to the sample are used as independent variable (*x*-axis), and as dependent variable (*y*-axis) the analytical signal obtained by monitoring different analyte emission lines in the mixture prepared by adding the diluent to the sample. Using least squares regression, a linear model is obtained, where the slope (angular coefficient) of the model can be obtained. Using the slope value obtained and the added (known) analyte concentration in the standard preparation, it is possible to determine the analyte concentration in the analyzed sample [59], as follows (Eq. 2.2):

$$\text{Concentration}_{\text{analyte}} = \frac{\text{slope} \times \text{added standard concentration}}{1 - \text{slope}} \tag{2.2}$$

Several applications are reported in the literature using LIBS for quantitative analysis and employing MEC as a calibration strategy. In food analysis, MEC was evaluated in the determination of Ca, K, and Mg in dietary supplements using microcrystalline cellulose as blank and binder; and performing a study of the influence of different concentrations of analytes added during the preparation of the standard containing sample:standard [61]. In two other studies, MEC-LIBS was evaluated in the analysis of solid mineral supplements for cattle to determine Ca, Cu, Fe, Mn, and Zn, using Na_2CO_3 as blank and 50:50 (w /w) ratio in the preparation of two standards required [60]. In the second study, the authors determined Ca and P using Na_2CO_3 as blank, 80:20 ratio (w /w) in the preparation of calibration mixtures. In addition, identifying an emission line of P I 253.39 nm interfered by the emission of Fe I 253.41 nm [31], both studies obtained satisfactory trueness in the range from 80 to 120%.

MEC was used for the determination of Cr and Ni in nickeliferous ores. Sodium carbonate (Na_2CO_3) was used as blank and diluent, and Cr and Ni nitrates as standards [62]. Carvalho et al. [63] determined Al, Fe, and Ti in high-silicon-content samples. In this study, a CRM containing the analytes was used to prepare the calibration sample, SiO_2 used as blank, and lithium borate flux used in the standards fusion procedure to obtain fused glass discs for LIBS analyses; in addition, B and Li emission lines were evaluated as IS [63].

Electronic waste was analyzed by LIBS to determine strategic, base, and rare earth elements (REE), present in the composition of electronic components and evaluating the advantage of matrix-matching via MEC. In the analysis of liquid crystal display from mobile phones to determine In, the two calibration samples required *per* sample in the MEC were prepared using SiO_2 as a blank and microcrystalline cellulose as a binder in the preparation of the pellets, and one of the five In emission lines monitored presented spectral interference, identified as outlier in the calibration model and removed from the model [64]. In another work, samples of exhausted computer hard disk magnets were analyzed to determine REE (Dy, Gd, Nd, Pr, Sm, and Tb) and base (B and Fe) elements of these components by LIBS. Due to the high Fe concentration (approximately 60% (w /w)) in these samples and

the several Fe emission lines with great potential to interfere with the REE emission lines, the two prepared standards used the ratio 42:58 (w /w) [58].

An iterative multi-energy calibration (IMEC) method was proposed by Li et al. [65] for online Ni-based alloy smelting process monitoring by LIBS. In this study, IMEC used four Al emission lines and an appropriate algorithm to propose the quantitative models. Thus, the potential of this calibration strategy in providing quantitative results with satisfactory analytical parameters in online LIBS applications was demonstrated.

2.4.2 One-Point and Multi-Line Calibration

As it is known from the Boltzmann equation, the emission intensity is proportional to the spectroscopic parameters of a given emission line, experimental constant, plasma temperature, and the concentration of analyte in the sample. In this context, the one-point and multi-line calibration (OPMLC), reported by Hao et al. in [66], proposes a linear calibration model monitoring several analyte emission lines in the sample with unknown concentrations and, only a single calibration sample for analyte determination by LIBS.

Similar to the MEC, in the OPMLC emission lines with different sensitivities are monitored for the proposition of the calibration model. However, in OPMLC only a single calibration sample is required for all samples with unknown concentrations analyzed. This calibration sample must present a matrix similar to all samples that will be analyzed to occur matrix-matching. In addition, the concentration of analytes in the calibration sample cannot be very different from the concentrations that are expected to be determined in the analyzed samples, if the concentration is much higher or lower, the accuracy of the determinations may be compromised [25, 66].

The linear OPMLC calibration model is obtained using least squares regression, with the independent variable (x-axis): intensity values monitoring the different analyte emission lines in the calibration sample, and as dependent variable (y-axis): the intensities values obtained by monitoring different analyte emission lines in the sample with unknown concentration. Figure 2.4 illustrates a linear OPMLC model.

From the slope obtained, and the known analyte concentration value, in the calibration sample, it is possible to determine the analyte concentration in the sample [66], as follows (Eq. 2.3):

$$\text{Concentration}_{\text{analyte}} = \text{slope} \times \text{standard analyte concentration} \tag{2.3}$$

OPMLC is a very interesting univariate calibration strategy to be evaluated in the elemental determination by LIBS in unknown samples that do not show great variability in analyte concentrations (e.g., in certain industrial processes). Furthermore, it is a very promising strategy in the development of analytical methods where

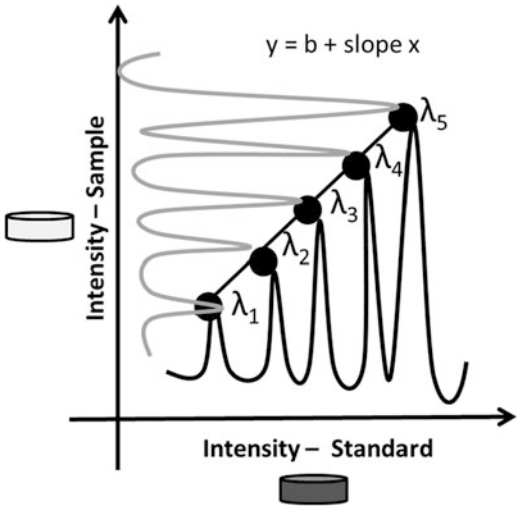

Fig. 2.4 Illustration of a linear OPMLC model monitoring five emission lines (λ) for an analyte in the sample and calibration sample

there are few samples available to be used in the set of calibration samples, as it requires a single calibration sample [25].

Some studies in the scientific literature report the use of OPMLC in the elemental determination by LIBS. In the introductory study of OPMLC [66], the authors determined Cr, Mn, Ni, and Ti in low-alloy steel samples, to minimize instrumental fluctuations in the acquisition of LIBS emission spectra, and they used Fe emission lines as internal standard. Thus, models with an acceptable coefficient of determination values ($R^2 \geq 0.8833$) were obtained for all analytes and, average relative errors for determination in the range from 9 to 36%.

In the direct determination of macronutrients Ca, K and Mg in cocoa seeds by LIBS using OPMLC, RSD values $\leq$26% were obtained for all analytes [67]. In the determination of Al and Pb in six waste printed circuit boards (PCB) samples, OPMLC models were obtained by monitoring four and two analyte emission lines, respectively. Root mean squared error of prediction—RMSEP values of 5.0 g kg^{-1} Al, 0.91 g kg^{-1} Pb and, RSD values $\leq$25% were obtained [24].

Furthermore, in the determination of P in fertilizers and Al in plant tissue, the authors used three P I lines at 213.62, 214.91, and 215.41 nm in the proposition of the OPMLC model [68]. However, for Al determinations, the authors used an interesting strategy to obtain the OPMLC model, using the emission intensities measured at five wavelengths located in the wing of the Al I emission line at 308.22 nm (308.01, 308.07, 308.12, 308.17, and 308.22 nm). This strategy was employed to overcome the limited number of interference-free Al emission lines.

2.5 Single-Sample Calibration

Obtaining a regression model from a previously selected set of calibration samples is the most common practice to further determine the analyte concentration in an unknown sample. However, in the single-sample calibration (SSC) proposed by Yuan et al. [69], a single calibration sample of a similar matrix to other samples is used to provide matrix-matching, which has reference values of the concentration of the analyte and other elements that constitute the standard to be used in the determination of the analyte. The simple correlation (Eq. 2.4) used to calculate the analyte concentration in the analyzed sample ($C_{analyte}$) considers the concentration and emission intensities of the analyte and n other elements monitored in the calibration sample ($C_{\text{standard analyte}}$, $C^n_{\text{standard element}}$, $I_{\text{analyte standard}}$ and $I^n_{\text{element standard}}$), in addition to the emission intensities of the analyte and n others elements monitored in the analyzed sample $\left(I_{\text{analyte sample}} \text{ and } I^n_{\text{element sample}}\right)$ [69]:

$$C_{\text{analyte}} = \frac{\frac{C_{\text{standard analyte}} \times I_{\text{analyte sample}}}{I_{\text{analyte standard}}}}{\sum_{i=1}^{n} \frac{C^n_{\text{standard element}} \times I^n_{\text{element sample}}}{I^n_{\text{element standard}}}} \tag{2.4}$$

Nevertheless, in SSC additional care must be taken to use emission lines free from spectral interference that will be used in the correlation [69].

2.5.1 Slope Ratio Calibration and Two-Point Calibration Transfer

Nunes et al. [70] proposed the slope ratio calibration (SRC) strategy, which is based on a single solid calibration sample. The fundamentals of the method are as follows. The analyte emission intensity (I) is directly proportional to the analyte amount in the ablated mass (m), where $I = k_1 \cdot m$; also being proportional to the number of laser pulses (N_p) in the case of signal accumulation via $m = k_2 . N_p$. Therefore, sample ablation efficiency (k_2) and analyte atomization/thermal excitation/optical efficiency of the system (k_1) can be described by a proportionality factor (K) between I and N_p ($I = K \cdot N_p$). In general, this strategy is related to the increase of the ablated sample mass with the number of accumulated laser pulses.

The single solid calibration sample can be a CRM or a reference sample with known concentration of the element of interest. In addition to that, an unknown sample with the element of interest is also used. Therefore, two linear models are built by plotting the analyte emission intensities (dependent variable) as a function of the number of laser pulses accumulated for both samples (independent variable).

The concentration of the analyte in the test sample (C_{sample}) is calculated according to the ratio between the slopes of standard (b_{std}) and the test sample

(b_{sample}) values and, the known analyte concentration in the standard (C_{std}) using Eq. 2.5:

$$C_{sample} = \frac{b_{sample}}{b_{std}} \times C_{std} \tag{2.5}$$

This strategy was evaluated for the determination of macro- and micronutrients in plant leaves with NIST 1547 as standard, using between 5 and 30 laser pulses *per* site for calibration. The accuracy was assessed from the analysis of CRMs and the comparison with the results by ICP-OES after microwave-assisted acid digestion, with agreement at the 95% confidence level.

Another interesting calibration method similar to SRC was proposed by Castro et al. [58], named as two-point calibration transfer (TPCT). It is derived from the SRC approach with only one difference: the models are calculated using two points (TP) of accumulated laser pulses. In TPCT only two sets of accumulated signals are used for sample with unknown analyte concentration and standards or reference samples (with known analyte concentration). Therefore, two linear models are obtained monitoring two analytical signals from set 1 and set 2.

In LIBS, hundreds of spectra are obtained for a representative analysis, so it is possible to obtain two sets of spectra and sum the spectral information from both. It is important that set 2 must be at least twice as large as set 1. As the model is calculated with two points, an *F*-test is performed to note the variances related to residues and the regression. Therefore, *F*-values are calculated from the MSR and MSr, if the $F_{experimental}/F_{tabulated}$ is ≥ 10 (p value <0.05), the model is considered valid statistically (regression is higher than and different of residue). The concentration of the analyte in the test sample is calculated equal to the SRC using Eq. 2.5.

This strategy was evaluated for the direct analysis of hard disk magnets with determination of REE. The accuracy was calculated using the reference concentrations (ICP-OES results) [58]. TPCT has also been successfully employed by Gamela et al. [67] in the determination of Ca, K, and Mg in cocoa beans, by Costa et al. [71] for the determination of Pb content in recycled polypropylene from car batteries and, by Babos et al. [24] for determination of Al and Pb in waste PCB.

A limitation of both strategies (SRC and TPCT) is the choice of the standard for calibration. The laser-sample interaction depends on the physicochemical characteristics of the sample (sample particle size, porosity, and density of the pressed pellets), the laser properties (wavelength, pulse duration, repetition rate, energy) and optical design (lens-to-sample distance). As the test sample and standard are measured using the same instrumental parameters, the accuracy in the calibration depends on the similarity between both samples (test and standard samples) for a perfect matrix-matching. In general, both strategies minimize the matrix effects, there is a simplicity in the data processing and, for the TPCT the linear model is built with two points being also an advantage over the SRC. Figure 2.5 shows a hypothetical example for both strategies.

Both SRC and TPCT are useful for homogeneous samples as those described in this section. In addition, it is always important to run confirmatory measurements

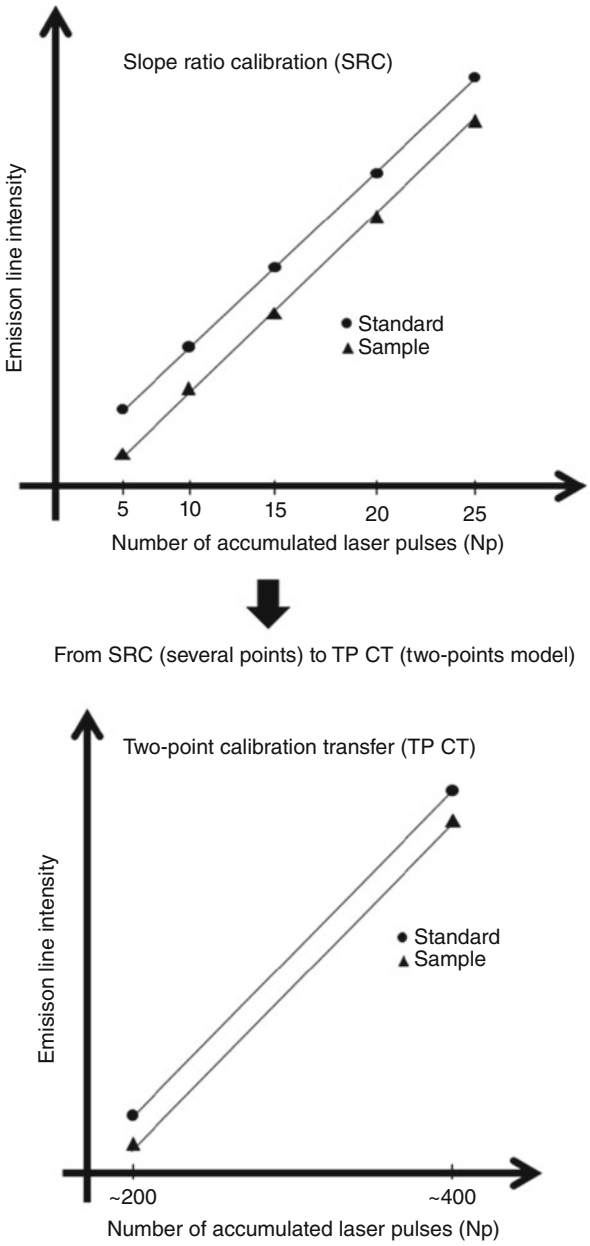

Fig. 2.5 Illustration of the concepts of the slope ratio calibration and two-point calibration transfer methods

using a reference technique as ICP-OES after proper sample preparation. As can be noted, these strategies are useful for routine analysis where the sample matrix only varies slightly.

2.5.2 Inverse Calibration

Generally, univariate calibration models used in LIBS employ simple linear regression to estimate the relationship between an independent and a dependent variable, which usually correspond to the concentration and the analytical signal, respectively [25]. Univariate calibration relates two variables, x and y, through a model to predict one variable based on the other in a second step. The direct model has been widely used to build quantitative models to predict absolute mass or concentration from an instrumental measure that employs spectroscopic techniques such as LIBS. A linear relationship between x and y can be considered from Eq. 2.6 [72]:

$$y_i = b_0 + b_i x_i + \varepsilon_i \tag{2.6}$$

where b_0 and b_i are the coefficients and ε_i, the error.

This model is often used in LIBS and it is called a direct model. The direct model's concentration is the independent variable, and the analytical signal is the dependent variable. In the direct model of y over x, the measures of x are assumed to be error-free. Duponchel et al. [73] evaluated direct and also inverse models for the determination of Ca in soils and Na in glasses. In the inverse model used by the authors, concentration is the dependent variable, and analytical signal is the independent variable. In the inverse linear regression of x on y, measurements of y are assumed to be error-free from Eq. 2.7 [72].

$$x = \beta_0 + y\beta_i + \varepsilon \tag{2.7}$$

When this inversion concerning the dependent and independent variables happens, the values of the intercept and slope of the analytical curve are different. When a test sample is analyzed, the predicted concentrations are different; it shows that the prediction of analyte concentration depends on the chosen model. In this study, the inverse model showed the lowest root mean square error of calibration (RMSEC) and RMSEP. Therefore, comparing direct and inverse models is interesting to find the best strategy for the considered data set. The authors also add that the smaller the signal-to-noise ratio (SNR), the greater the differences. Additionally, researchers are advised to use the inverse models when the number of calibration samples is low.

2.5.3 Fluence Calibration

Different non-traditional calibration strategies were already presented here. It could be observed that among the novel calibration methods, MEC uses several emission lines for the acquisition of analytical signal and OPGSA, SSC, SRC and TPCT use one or two calibration samples to build a calibration curve or linear model [25], but what happens if an instrumental parameter could be used to develop a calibration strategy?

In this sense, fluence calibration (FC) was developed to minimize matrix effects for quantitative LIBS analysis. Laser pulse fluence is an important instrumental parameter in LIBS, because the efficiency of the laser-sample interaction and the vaporization, atomization, ionization process is also dependent on this parameter [74].

Laser (pulse) fluence is the laser energy delivered *per* unit area (J cm^{-2}) and when the fluence value is increased, the plasma temperature also increases, a larger amount of sample is ablated and more analytes are vaporized, atomized, ionized into the plasma [14, 74]. Taking into consideration this relationship between laser pulse fluence and sample mass ablated, FC was developed.

Fluence calibration is based on the use of a single calibration sample (as other aforementioned non-traditional calibration methods) to obtain a linear model at two different laser fluences. Then pellets of this single calibration sample (with the known concentration of the analyte) and of the samples are measured at the same two laser fluences. Authors emphasized that during the application of this FC method, the change of laser fluence has to be obtained via varying the laser pulse energy besides keeping the laser spot size fixed. The linear model is obtained from the emission signals plotted in the *x*-axis (signals obtained for calibration sample, independent variable) and in the *y*-axis (signals obtained for samples with unknown concentrations, dependent variable) and, from Eq. 2.8 it is possible to calculate the analyte concentration:

$$C_{\text{sample}} = \text{slope} \times C_{\text{standard}} \tag{2.8}$$

where C_{sample} is the analyte concentration determined in the sample, slope value is obtained from the linear model and C_{standard} is the known analyte concentration in the calibration sample [75].

In the FC method, both standard and sample are exposed to different laser pulse fluences, i.e., different plasma conditions and this exposition lead to similar plasma conditions for both standard and sample (and of the process that occurs in the plasma as vaporization, atomization, and ionization) which is one of the factors responsible for minimizing matrix effects and ensure accuracy and precision of the results [75].

The first paper reported in the scientific literature combining FC and LIBS (FC-LIBS) by Machado et al. [75]. In this study, the authors evaluated the performance of FC for the determination of Al and Pb in PCB waste and Al, K, Mg, Na, and P in fertilizer samples. The laser fluence values were optimized for each sample matrix and spot size was fixed at 50 μm. The best combinations were achieved using 2546 J cm^{-2} and 4074 J cm^{-2} for PCB samples and 2546 J cm^{-2} and 4584 J cm^{-2} for fertilizers samples. In several LIBS instruments, it is easily possible to prepare laser conditions with different setups in order to obtain distinct fluences. Using these optimized fluences, excellent accuracy and precision results were obtained during the analysis of PCB and fertilizer samples. The selection of the calibration sample was an important aspect to be considered to reach adequate accuracy and precision

using FC-LIBS. Moreover, considering the linear model with two-point, *F*-test was calculated for each model to evaluate its significance (as previously described).

It was observed that depending on matrix complexity, the performance of the calibration method depends on physicochemical properties and the analyte concentration in the calibration sample and samples. The authors also evaluated FC without a matrix-matching approach, using calibration sample prepared mixing salts for PCB and fertilizer samples. Even considering the absence of sample matrix in the calibration sample, good accuracy and precision were obtained for Al in two PCB samples and Al and P in two fertilizer samples. It is completely desirable to have a universal standard for calibration, but for strategies that use only one standard, factors such as different elements, their concentration (in the standard and samples), and sample matrix can influence the obtaining of satisfactory results. Therefore new FC-LIBS applications may bring more knowledge about the influence of these factors in the accuracy of the results. It is important to highlight the FC advantages, such as the capability to overcome matrix effects, simplicity, faster pellet preparation (use of only one calibration sample), fast data acquisition, and data treatment for the direct analysis of complex solid samples.

As a final remark in this section about non-traditional calibration strategies, the LIBS user can first test MEC to verify the presence of spectral interference on the emission lines selected for the determination of the analyte. These lines can be removed if the interference is confirmed. Then, other strategies can be also tested as OPMLC, SRC/TPCT, or FC. Furthermore, it is important to mention that some strategies, such as TPCT, assume a linear relationship between the analyte signal and its concentration. In this case, some confirmatory determinations must be performed using reference techniques such as ICP-OES. Another aspect to be emphasized is the fact that these nontraditional calibration strategies are very useful for routine analysis (in metallurgical applications, for instance) where the sample matrix is stable and well known.

2.6 Multivariate Calibration

Multivariate calibration tools have been widely applied in LIBS to improve the accuracy of quantitative analysis [25, 76]. This type of calibration is used when an element cannot be determined with only one parameter obtained from the spectral data [77]. Multivariate calibration has some advantages such as (1) it can take full use of LIBS spectral information and improve the precision and accuracy of the measures; (2) it is possible to determine the analyte in the sample even in the presence of the interferent, since the interferent is also included in the calibration model [25]. The most popular multivariate calibration methods for LIBS quantitative analysis involve multiple linear regression (MLR), principal component regression (PCR), partial least squares (PLS), and artificial neural networks (ANN) [25]. It is

important to mention that multivariate calibration is unable to solve all analytical problems, but can bring useful applications, as can be noted in the next lines. According to the Web of Science, since 2010, the number of publications on LIBS analysis with multivariate calibration has been increasing significantly, and among the methods mentioned, PLS is the most widely used, as shown in Fig. 2.6.

2.6.1 Multiple Linear Regression

The aim of MLR is to model the linear relationship between a dependent variable (response) and multiple independent variables by regression functions. In MLR, the interferents, impurities, and effects of baseline are treated without problem if they are present in all samples in the calibration dataset. On the other hand, a huge limitation is the number of variables, and this number should be lower than the number of samples to enable the calculation of matrix inversion to obtain the regression vector. Thus, it is necessary to make a variable selection and choose some emission lines for the target element. Moreover, for a good model, besides the limitation of the number of variables, these chosen variables cannot have a huge correlation among them, because this can also cause difficulties in the matrix inversion [78].

In a study by Ayyalasomayajula et al. [79], LIBS and MLR were used to quantify the total carbon concentration in soil. For the variable selection, the authors employed the ratio of C (247.48 nm) with Fe lines (246.51 and 247.48 nm). The results showed that the LIBS and MLR combination can be successfully applied to the quantitative measurement of C in soil with a small error. Wang et al. [80] assessed univariate (MMC and IS) and multivariate (MLR) calibration strategies to determine Pb in tea leaves by LIBS. The MLR presented better quantitative performance than the other two univariate strategies. As mentioned before, the MLR models use more information to predict the concentrations of the element of interest improving the performance of quantitative analysis by LIBS.

Sperança et al. [81] determined Ti in sunscreen using LIBS, where several calibration strategies were applied, being MLR the best option (according to reference values provided by ICP–OES analysis). The authors selected two titanium emission lines: Ti I 498.17 nm and Ti I 499.11 nm. Other applications with good results using MLR and LIBS include the determination of elemental impurities in plastic [82] and determination of P in fertilizer [83].

2.6.2 Principal Component Regression

PCR is a regression based on the same decomposition as PCA. First, PCR decomposes matrix $\mathbf{X}$ with n samples and p pixels or variables (in this case, the number of emission lines recorded in a LIBS spectrum). After this decomposition, the scores and loadings are used to calculate the regression coefficients b for the prediction of a vector $\hat{y}$ with n rows, that is, each row will correspond to a predicted concentration of the element of interest. PCR and PLS have similar mathematics

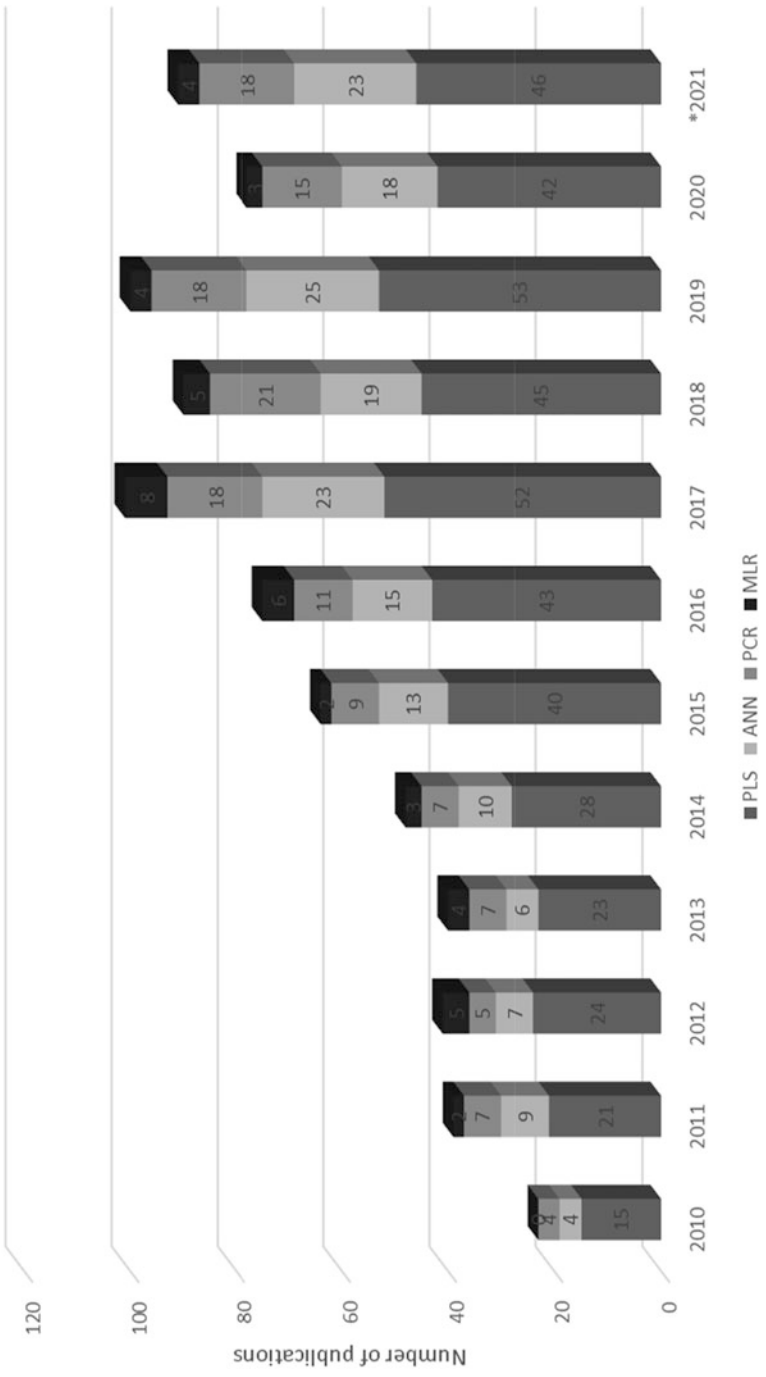

Fig. 2.6 Evolution of the number of LIBS publications using different multivariate calibration strategies (data for the year of 2021 is incomplete)

involved, hence the performance of these tools tends to be also similar. The main difference is that PCR does not relate the scores of matrix **X** with the concentrations, while PLS connects the **T** scores of **X** with the **U** scores of vector *y* [76, 78]. A lowercase letter means vector. Due to similar mathematics of PCR and PLS, the performance of both models is compared in many studies [25, 76].

PCR has already been used in combination with LIBS for the determination of Pb in recycled polypropylene from car batteries [71], to the analysis of Fe in iron ore [84], to the determination of Cr, Mn, Ni, and Si in high-alloyed stainless steels [85], among others [25]. Devangad et al. [86] determined Mn in glass matrices combining PCR. In this study, PCR models reached optimum method LOD and RMSEP of 0.02 and 0.54 w/w%, respectively, in a set of samples with a Mn concentration ranging from 0.77 to 11.61%. Takahashi et al. [87] used PCR to quantify the composition of brass alloys submerged in water using LIBS. The authors determined Cu and Zn, and PCR showed an RMSEP of 2.7 and 2.8%, respectively.

2.6.3 Partial Least Squares

PLS is a regression method that uses a selected number of latent variables to decompose the matrix **X** (independent variables) with *n* samples and *p* variables as well as the vector y (dependent variables) with *n* rows (reference concentration). The parameters of PLS can be obtained using calibration sample set, and there is no matrix inversion involved in the calculation, hence it has only a calculation error, thus high accuracy, fast execution, and a good predictive ability [77].

PLS tool is a powerful chemometric algorithm for multivariate calibration, but several important details must be observed for its correct application. The first, and more general one, is the overfitting when too many latent variables are used, showing a strong capability of predicting the concentrations of the samples used in the calibration, but the poor capability of predicting an unknown sample. In the case of PLS, the number of latent variables is optimized through cross-validation, and this helps to avoid under- or overfitting [77]. Another problem, not much reported but can occur, is present when the regression vector incorrectly correlates emission lines of elements. For instance, the algorithm correlates emission lines from Ca to predict Al concentration. It is, therefore, advisable for the analyst to examine the regression vector and confirm the correctness of the information [25].

In terms of application, PLS is employed to the most diverse types of samples in combination with LIBS including ceramics [88], polymers [71, 89], alloys [50], hard disk magnets [58, 90], medicinal herbs [91], among others [25, 76]. In this sense, Goueguel et al. [92] proposed PLS calibration models along with full LIBS spectra to predict soil texture (clay, silt, and sand percent). The authors reached prediction errors of 10% for sand and 3% for clay using PLS-based calibration models.

In a study published by Costa et al. [93], polycarbonate (PC) and acrylonitrile-butadiene-styrene (ABS) concentrations in blends from waste electrical and electronic equipment (WEEE) were determined. The authors prepared a calibration

curve using 11 calibration solid standards with a varying PC/ABS concentration in 10 w/w% steps. The predictive capability of PC and ABS using PLS models in this application showed standard error of cross-validation to be 5.6%. The prediction of concentrations was confirmed using differential scanning calorimetry (DSC).

Ding et al. [94] determined potential toxic elements (Cu, Zn, Cr, and Ni) in soil employing interval PLS (iPLS). This strategy divides the whole spectrum into n intervals and evaluates each one separately to detect which part is more accurate for the prediction of the concentration of analytes. In this study, the authors divided the full spectrum into 10–90 subintervals, varying from 10 to 100 emission lines. Compared to the PLS model using the full spectrum, the iPLS model showed a higher coefficient of determination values (R^2) and lower prediction error for Cu, Zn, Cr, and Ni.

2.6.4 Artificial Neural Networks

Comprehension, reasoning, perception, communication, and learning are some capabilities of ANN, imitating the structure of a human brain. This method can handle nonlinear, noisy, or imprecise data quite well. It is a nonlinear functional mapping between an input and an output data space. This network operates using a large number of "neurons" (parallel-connected simple arithmetic units), which can be defined as a nonlinear, parameterized, and bound function (examples include sigmoidal and Gaussian functions). The neurons operating on the same input variables are organized in layers, while the weights (combination of the nonlinear functions) are represented as lines, connecting units in different layers. There are three types of layers: input, hidden, and output. The input layer is the data given to the network, the hidden layer is the intermediate computation, and the output layer is the response relative to the input. Therefore, the aim of the neural network is to transform the inputs into meaningful outputs, extracting important features [76, 78, 95].

In the case of LIBS, the inputs are spectra. The ANN models are optimized to obtain the best representation of the output set (concentration of analyte) with a number of known samples (training set). In the training dataset, there is a set of inputs with their respective desired outputs. A function modifies the weights of the network until the resultant error is less than a predefined error, so the network infers a relationship between the inputs and outputs. With this relationship, the ANN can make predictions for an unknown sample [96].

Ferreira et al. [97] determined Cu in soil samples using ANN as calibration strategy for LIBS. The variable selection (for ANN training) was made by simple linear regression and wrapper performance in order to select the wavelengths with the best linear correlation with Cu. ANN used a multilayer perceptron (MLP) and the results presented good accuracy, proving to be an efficient strategy for Cu determination in a heterogeneous set of soil samples. Other studies related to soil analysis and LIBS using ANN as calibration strategy have also been reported in the literature [98–100].

Another application in the literature is with the metallic alloys [101–103]. In this sense, Inakollu et al. [104] performed a comparative study between traditional and ANN calibration for the analysis of different Al alloys by LIBS. The authors used some emission lines for the elements of interest (Cu, Cr, Mg and Mn) and, besides that, they also used the intensity ratio of the spectral lines of these elements compared to an Fe line. In this case, the concentration of the element relative to a reference element (Fe, as an example) can be found. In 75% of the cases, the predicted concentration values using the intensity ratio of the elements by ANN presented better results than the traditional calibration, with values closer to those determined through reference method.

In a recent study with forensic nuclear materials, LIBS and ANN were applied jointly by Bhatt et al. [105]. The authors used LIBS in air at atmospheric pressure for the quantification of trace levels of uranium in cellulose (in order to mimic a typical scenario of illicit nuclear and radiological material) and uranium-bearing mineral ores. The multivariate calibration using ANN (using the back-propagation algorithm) was successfully employed using weak and resonant uranium lines. Other studies dedicated to ANN and LIBS were applied to online measurement for the gross calorific value (GCV) of coal [106], quantitative determination of Ca, K, and Mg in the roots [107], and in the determination of trace elements in geological samples [108].

2.6.5 Calibration Based on Linear Correlation

In 2001, Galbács et al. introduced a new calibration method based on spectrum comparison using the linear correlation formula (linear correlation calibration method, LCM) [109]. This method can be advantageously applied to all multi-component solid samples containing chemical constituents in comparable concentrations (minor and major components). The LCM method produces a calibration plot with the value of the linear correlation coefficient on the *y*-axis calculated by the comparison of the spectrum of one of the components in the sample in the pure form to the spectrum of a series of calibration samples containing the analyte at various relative concentrations (e.g., on the *x*-axis, the mass fraction of the analyte would run from 0 to 100%). It was shown that the calibration curve produced in this way will always be monotonous and monovalent and that it can be very well fitted with a quadratic or cubic polynomial function. The method can be simply extended to multi-component (N) samples, by producing the calibration curves for $N\text{-}1$ components.

The main advantage of the LCM method is that given the complete immunity of the linear regression coefficient to the linear transformation of any of the involved datasets (samples or standards), the calibration curves can be stored and used for a long time, e.g., in portable instruments. It is important to consider that in most cases, an instrumental drift or aging will result in the change of sensitivity or background, hence affecting the data by a near-linear transformation. The analytical precision and accuracy are also largely improved, thanks to the fact that the calibration is based on

the complete spectrum, not, e.g., only the intensity of a single spectral line. It was shown that the repeatability of the data points in the calibration plot is at least ten times better than with univariate calibration.

The LCM method was first developed and demonstrated for LIBS, applied to the accurate analysis of various alloys (e.g., brass, aluminum alloys, gold alloys, etc.) [109, 110]. Later, the same research group extended the applicability of the method to trace analysis of solid and liquid samples by the transformation of the *x*-axis. This extended version of the method was called Generalized Linear Correlation Method (GLCM) and was successfully demonstrated to work not only for LIBS, but also for UV-Vis absorption spectroscopy and ICP-MS [111]. The relative error in concentration determination generally ranged from 0.1% to 5%.

2.6.6 Data Fusion

With the fast development of new chemical analysis procedures, along with modern high-throughput technologies, the data generated has been increasingly larger, complex, and multivariate. The era of big data poses difficulties for extracting value information from a huge volume of data and, according to Meng et al. [112], they are related to "5 V" characteristics: volume, variety, velocity, veracity, and value [112].

In the cases of chemically rich samples, a single measurement method can be unable to extract all the useful information. Combining data from complementary analyses is an alternative way to enhance the extracted knowledge about sample features. In practice, however, increasing availability of multiple data using different acquisition methods brings new challenges to traditional data processing methods that assume independent variables [113]. Indeed, conventional statistical methods are unable to produce reliable, valuable, and accurate information from massive data. On the other hand, besides the information explosion, modern technologies introduce us to several data processing methods to obtain more informative, objective, and accurate information than the original big data [112].

There is always much interest from the scientific community in gathering heterogeneous information systems through a consistent data integration interface. Chemometrics has proven to be a powerful tool in data science for grouping convergent outputs as well as for retrieving hidden chemical information in multivariate data [113, 114]. Data fusion is a method of concatenating multiple blocks of data from different records into a single, consistent, and clean representation [115].

Ways of the successful implementation of data fusion may differ from system to system, due to the various levels of complexity. Three main possibilities are generally explored: low-, mid-, and high-level data fusions [116]. These approaches are similar, differing mainly in the treatment stage of each data source aligned to standardization, preprocessing, and variable selection (if necessary). The choice of the best method to be performed depends on the goal, measurement procedures used, sample matrix, volume, and type of data to combine. The simpler approach is the low-level method that assumes the direct fusion of multiple raw data to obtain a

regression model. Limitations reported for this method include big data sets and predominance of one data over other measure systems. In this case, mid-level data fusion brings the solutions to these limitations, in which it first extracts the relevant features from each data source individually and then these variables are merged into a single matrix. The reduction of the data array and selection of important variables from each data block facilitates the interpretation of the results and the visualization of the contribution from each fused measure source. Finally, the method known as high-level data fusion is accomplished at the decision results obtained from multiple data sets to produce a unique solution [116–118].

Chemometric techniques have been indispensable in the progression of data fusion methods and in the search for quality data. For instance, descriptive models using PCA are carried out for a preliminary exploratory analysis. Classification models include linear discriminant analysis (LDA), k-nearest neighbors (kNN), soft independent modeling of class analogy (SIMCA), partial least squares discriminant analysis (PLS-DA), and supervised learning algorithms such as support vector machine (SVM) and ANN. For the prediction purpose, PLS is the most sought-after method, but other less popular approaches have been investigated, including PCR, MLR, and SVM regression [116].

Data fusion is a relatively novel subject in LIBS analysis, and it has been increasingly applied to the qualitative and quantitative analysis of a variety of matrices. In the concern about food authenticity and classification, LIBS was combined with UV-Vis absorption spectroscopy for the discrimination of 41 Greek olive oils based on their cultivar origin. LDA and gradient boosting algorithms were used to create the prediction models and found to provide excellent classification, resulting in a 96% training accuracy and 94% for external validation [119]. In the same respect of food analysis, Gamela et al. [120] assessed the complementary information of LIBS and wavelength dispersive X-ray fluorescence (WDXRF) for the macronutrients determination in bean seed samples. The data fusion strategy in the low level was proposed using MLR and leave-one-out cross-validation. This method showed a lower standard error of cross-validation (SECV) and better accuracy, precision, and robustness compared to those univariate calibration models for each technique individually [120]. Gamela and coworkers also reported the combination of LIBS and energy dispersive X-ray fluorescence (EDXRF) using PLS chemometric technique for low-level data fusion [121]. The concentrations of K were determined in cocoa beans ranging from 6053 to 8339 mg kg^{-1}, and the proposed model presented good results, as low SECV (0.09%), LOD (0.2%), and acceptable trueness (85–120%).

LIBS and XRF techniques were also combined and used in monitoring the chemical composition of electronic waste samples. Andrade et al. [122] proposed the determination of Cu in 40 fragments of PCB samples, and low-level data fusion was run using PLS regression. The results were compared with the reference concentrations (ranging from 13 to 45% w w^{-1} Cu) obtained after microwave acid extraction and ICP-OES determinations, and the trueness was in the range of 81 to 119% using leave-one-out cross-validation [122]. Other applications including the information from LIBS and XRF techniques were reported for the direct analysis of

human hair samples [123]. A total of 127 samples were evaluated using both analytical techniques, and data fusion was used to build a classification model. The authors proposed the combination of 17 classifiers, that is PLS-DA, kNN, the Mahalanobis distance (MD), sinθ, cosθ, Q-residual (Q res), divergence criterion (DC), the Euclidean distance, determinant, inner product correlation, unconstrained Procrustes analysis (PA), constrained PA (for 2 classifiers), and the extended inverted signal correction difference (EISCD) (for 4 classifiers). The data fusion improved the figures of merit for the classification, confirming that LIBS and XRF spectral features are complementary to each other. The method trueness ranged from 99.2 and 100% in comparison with 94.5–99.2% for WDXRF and 99.2% for LIBS, individually.

Studies have been reported using LIBS combined to other spectroscopy techniques. Of particular interest in environmental analysis, outputs from LIBS and near-infrared spectroscopy -NIRS were combined to produce regression models. In a study published in 2019 de Oliveira et al. [124] assessed the inorganic composition of forage plants, and data fusion models for Ca, Fe, K, Mg, and Mn using PLS showed better figures of merit than any of the two individual techniques [124]. Using the same two techniques coupled with XRF and mid-infrared spectroscopy (MIR), Xu et al. [125] proposed a multi-sensor fusion for monitoring several soil properties such as soil organic matter (SOM), pH, total N, available K, and available P. The prediction capability of data was assessed using different combinations decreased as follows: MIR > NIR > LIBS > XRF [125, 126] assessed the detection of SOM content by LIBS and Fourier transform mid-infrared (FT-IR). This study demonstrated the combination of these complementary techniques using various chemometric algorithms (i.e., PCA, PLS, SVR, and ANN). The quantitative prediction ability of the method was assessed using a low-level and mid-level data fusion. The findings from SVR, ANN models indicate that either calibration strategies are promising for monitoring organic matter in soil samples. Nevertheless, mid-level data fusion of the LIBS and FTIR-ATR spectra based on the latent variables of PLS drastically improved the SOM prediction accuracy [126].

Interestingly, Manrique-Martinez et al. [127] proposed the strategy of data fusion between LIBS and Raman for the investigation of samples in binary mixtures, as a part of simulation in planetary exploration missions. Two different sulfates (epsomite and anhydrous sodium sulfate) and a chloride (hexahydrate magnesium chloride) were used to prepare 27 binary mixture combinations. These samples were analyzed using both techniques and multivariate analysis was performed on Raman, LIBS, and Raman combined with LIBS using low-level fused data sets. As demonstrated in other studies, data fusion method showed better analytical performance and more accurate results when compared with individual sets [127].

2.6.7 Other Multivariate Approaches

The literature also presents other calibration and exploratory analyses using LIBS. For instance, Araújo et al. [128] proposed a method for Ca, K, and Mg determination

in human mineral supplements and Al, Cu, and Fe in PCB using unfolded-PLS with residual bilinearization (U-PLS/RBL). Castro et al. [90] used parallel factor analysis (PARAFAC) for spectral interference identification and removal focusing WEEE [129] precious elements (Ag and Au) determination.

2.7 Hyperspectral Images

The principle of hyperspectral imaging is based on the fact that all materials, due to the difference in their chemical composition and inherent physical structure, reflect, scatter, absorb and emit electromagnetic energy in distinct patterns at specific wavelengths. This feature is called a spectral signature or spectral fingerprint, or simply spectrum. A spectral signature is a unique feature of an object. For a given material, if the percentage of reflectance, absorbance, or transmittance, is plotted against wavelengths, the resulting curve is referred to as the spectral signature of that material. In essence, the spectral signature can be used to characterize, identify and discriminate between classes of any materials in each pixel of the image [130].

According to Wu and Sun [131], the spectral hypercube is composed of voxels (also called vector pixels) containing spectral information (of λ wavelengths) and also bi-dimensional spatial information (of x lines and y columns). Thus, the hyperspectral cube consists of a series of contiguous sub-images one after the other at different wavelengths, so each sub-image provides the spatial distribution of the spectral intensity at a given wavelength. This means that a hyperspectral image described as $I(x,y,\lambda)$ can be seen as a separate spatial image $I(x,y)$ at each individual wavelength or as a spectrum $I(\lambda)$ at each individual pixel (x,y) [139]. Thus, this technology allows, through the generation of concentration maps, the determination of the local composition of the species of interest throughout the spatial structure of the sample. With this local description of chemical information, it is possible to obtain, for example, data on the homogeneity and distributions of constituents and to interpret and monitor processes that may occur on the surfaces of certain samples. Furthermore, the use of spectral images has proved to be an important tool for the acquisition of chemical information in non-homogeneous media and its main advantage is the minimum preparation and handling of samples.

A hyperspectral image can be formed by hundreds of thousands of measurements and one of the main problems with this approach is the requirement to process so much data without a minimal loss of quality and quantity of information. In the case of the LIBS technique, each pixel corresponds to an emission spectrum, and since there are LIBS spectrometers that have the ability to monitor thousand wavelengths, which will generate the same number of emission spectra matrices. The use of data compression techniques such as PCA may satisfactorily solve this problem [132].

The use of hyperspectral images in chemical analysis began in the 1970s, mainly with applications in remote sensing; however, it was only many years after, this tool started to be used in several other different applications such as pharmaceutical research and production, food science, food quality assurance, forensic science, biochemistry and biomedicine, cultural heritage, among others [133]. In the case

of forensic science, hyperspectral imaging can allow investigators to analyze chemical composition and simultaneously visualize the spatial distribution of a given sample at a crime scene. According to Edelman et al. [134], recent technological developments in fast, portable, and high-resolution acquisition systems, such as LIBS, are facilitating the use of hyperspectral images in forensic science, since, in most cases, it is possible to obtain chemical information with little sample manipulation and, in addition, the acquisition of spectra can be performed in the field, minimizing the need to take the sample to a laboratory [134].

Another interesting application of LIBS with hyperspectral imaging was reported by Wu et al. [135]. In this work, the authors developed a fast and efficient way to detect pesticide residues (thiophanate-methyl) in mulberry fruits. PCA and PLS were used to qualitatively and quantitatively analyze the data obtained from fruit samples with different concentrations of thiophanate-methyl. The authors conclude that the use of LIBS technology in combination with hyperspectral images for the detection and identification of residues of the thiophanate-methyl pesticide is feasible, and the best results were provided by the PLS model using optimal pre-processed variables [135].

Therefore, spectral images prove to be a promising, efficient, and reliable technology, which can be used, in conjunction with LIBS [136], to replace other analytical methods, especially in situations where the sample cannot be fully consumed, such as in forensic analysis. By combining spatial and spectral details in one data set, the hyperspectral imaging technique can simultaneously acquire spatial images in many spectrally contiguous bands to form a 3-D hyperspectral cube, and it is considered to have the ability to complement the advantages of spectroscopy and imaging techniques. Predicted values of pixel-level quality or safety attributes can then be used to generate the attribute distribution map, leading to better characterization and better quality and safety assessment results. Currently, there are still many challenges to be tackled, e.g. computing speed, hardware limitations, and high cost before this techniue can be fully exploited. At present, spectral imaging studies often aim at identifying optimal wavelengths for designing a low-cost multispectral imaging system.

2.8 Conclusions and Perspectives

The use of LIBS in the direct quantitative analysis of several types of samples is promising, as the previous steps of sample preparation and handling are considerably simplified. However, the challenges related to the calibration of the obtained signals require special attention from the analyst and strategies aimed at matrix compatibility can be employed, sharply reducing the matrix's contribution. Due to the prevalence of LIBS, several review articles have been published on this topic [137]. A review of calibration strategies used in conjunction with LIBS was published by Costa et al. [25]. An important review was published by Lazic and Jovicevic [138] to present sample preparation strategies for liquid samples designed for quantitative determinations. Jantzi et al. [139] presented a complete review addressing

pretreatments of solid samples aimed at qualitative and quantitative analyses in 2019. In the same year, Costa et al. [140] also published a review on this topic, in which the authors addressed many aspects of LIBS, including history, fundamentals, sample preparation, chemometrics, and the application of LIBS in various fields of science [140].

The circle of LIBS applications is already vast and is still growing fast in the last decade. The outlook for the application of LIBS in industrial processes and product monitoring is very promising. In addition, it is possible to obtain point information from extremely small samples. An important aspect to emphasize is the fact that the information obtained using LIBS has a potential to cooperate with other instrumental techniques. LIBS, for instance is able to detect all elements from light ($Z < 11$) to heavy ones and can be used to analyze practically any type of solid samples (conductive or not) in several challenging conditions (e.g. space or underwater exploration). In addition, as a huge amount of data is collected it is mandatory in several cases to use chemometric tools in order to better exploit the data collected and to identify and eliminate signals from concomitants.

References

1. Nascentes CC, Korn M d GA, Zanoni MVB. Química Analítica No Brasil: Atualidades, Tendências E Desafios. Quim Nova. 2017;40:643.
2. Carter JA, Barros AI, Nóbrega JA, Donati GL. Traditional calibration methods in atomic spectrometry and new calibration strategies for inductively coupled plasma mass spectrometry. Front Chem. 2018;6:504.
3. Krug FJ, Rocha FRP. Métodos de Preparo de Amostras Para Análise Elementar. 2nd ed. São Paulo: EditSBQ; 2019.
4. Rocha DL, Batista AD, Rocha FRP, Donati GL, Nóbrega JA. Greening sample preparation in inorganic analysis. TrAC Trends Anal Chem. 2013;45:79.
5. Meyers RA. Encyclopedia of analytical chemistry: applications, theory and instrumentation, supplementary volumes S1–S3. New York: Wiley-Interscience; 2011.
6. Smith FE, Arsenault EA. Microwave-assisted sample preparation in analytical chemistry. Talanta. 1996;43:1207.
7. Radziemski LJ. From LASER to LIBS, the path of technology development. Spectrochim Acta B. 2002;57:1109.
8. Noll R. Laser-induced breakdown spectroscopy: fundamentals and applications. Springer Science & Business Media; 2012.
9. Pereira FMV, Castilho JPC, Machado RC, de Araújo AS, de Andrade DF, de Babos DV, Beletti DR, Pereira Filho ER, de Mello ML, Hilário FF, Garcia JA, Sperança MA, Gamela RR, Costa VC. Laser-induced breakdown spectroscopy (LIBS): applications and calibration strategies. 1st ed. São Paulo; 2021.
10. Pedarnig JD, Trautner S, Grünberger S, Giannakaris N, Eschlböck-Fuchs S, Hofstadler J. Review of element analysis of industrial materials by in-line laser—induced breakdown spectroscopy (LIBS). Appl Sci. 2021;11:9274.
11. Radziemski L, Cremers D. A brief history of laser-induced breakdown spectroscopy: from the concept of atoms to LIBS 2012. Spectrochim Acta B. 2013;87:3.
12. Machado RC, Andrade DF, Babos DV, Castro JP, Costa VC, Sperança MA, Garcia JA, Gamela RR, Pereira-Filho ER. Solid sampling: advantages and challenges for chemical element determination—a critical review. J Anal At Spectrom. 2020;35:54.
13. Cremers DDA, Radziemski LJ. Handbook of laser-induced breakdown spectroscopy. 2nd ed. Chichester, West Sussex: Wiley; 2013.

14. Hahn DW, Omenetto N. Laser-induced breakdown spectroscopy (LIBS), part II: review of instrumental and methodological approaches to material analysis and applications to different fields. Appl Spectrosc. 2012;66:347.
15. Singh VK, Rai AK. Prospects for laser-induced breakdown spectroscopy for biomedical applications: a review. Lasers Med Sci. 2011;26:673.
16. Galbács G. A critical review of recent progress in analytical laser-induced breakdown spectroscopy. Anal Bioanal Chem. 2015;407:7537.
17. Takahashi T, Thornton B. Quantitative methods for compensation of matrix effects and self-absorption in laser induced breakdown spectroscopy signals of solids. Spectrochim Acta B. 2017;138:31.
18. Popov AM, Zaytsev SM, Seliverstova IV, Zakuskin AS, Labutin TA. Matrix effects on laser-induced plasma parameters for soils and ores. Spectrochim Acta B. 2018;148:205.
19. Lednev VN, Grishin MY, Sdvizhenskii PA, Asyutin RD, Tretyakov RS, Stavertiy AY, Pershin SM. Sample temperature effect on laser ablation and analytical capabilities of laser induced breakdown spectroscopy. J Anal At Spectrom. 2019;34:607.
20. Sabsabi M, Cielo P. Quantitative-analysis of aluminum- alloys by laser-induced breakdown spectroscopy and plasma characterization. Appl Spectrosc. 1995;49:499.
21. Santos D, Nunes LC, Carvalho GGA, Gomes MD, Souza PF, Leme FD, Santos LGC, Krug FJ, L. Laser-induced breakdown spectroscopy for analysis of plant materials: a review. Spectrochim Acta B. 2012;71–72:3.
22. Braga JWB, Trevizan LC, Nunes LC, Rufini IA, Santos D, Krug FJ. Comparison of univariate and multivariate calibration for the determination of micronutrients in pellets of plant materials by laser induced breakdown spectrometry. Spectrochim Acta B. 2010;65:66.
23. Wang W, Sun L, Zhang P, Chen T, Zheng L, Qi L. Study of matrix effects in laser-induced breakdown spectroscopy by laser defocus and temporal resolution. J Anal At Spectrom. 2021;36:1977.
24. Babos DV, Cruz-Conesa A, Pereira-Filho ER, Anzano JM. Direct determination of Al and Pb in waste printed circuit boards (PCB) by laser-induced breakdown spectroscopy (LIBS): evaluation of calibration strategies and economic—environmental questions. J Hazard Mater. 2020;399:122831.
25. Costa VC, Babos DV, Castro JP, Andrade DF, Gamela RR, Machado RC, Sperança MA, Araújo AS, Garcia JA, Pereira-Filho ER. Calibration strategies applied to laser-induced breakdown spectroscopy: a critical review of advances and challenges. J Braz Chem Soc. 2020;31:2439.
26. Andrade DF, Pereira-Filho ER, Amarasiriwardena D. Current trends in laser-induced breakdown spectroscopy: a tutorial review. Appl Spectrosc Rev. 2021;56:98.
27. Musazzi S, Perini U, editors. Laser-induced breakdown spectroscopy: theory and applications, vol. 182. Berlin: Springer; 2014.
28. Mark H. Principles and practice of spectroscopic calibration. 1st ed. New York: Wiley-Interscience; 1991.
29. Donati GL, Amais RS. Fundamentals and new approaches to calibration in atomic spectrometry. J Anal At Spectrom. 2019;34:2353.
30. Augusto AS, Barsanelli PL, Pereira FMV, Pereira-Filho ER. Calibration strategies for the direct determination of Ca, K, and Mg in commercial samples of powdered milk and solid dietary supplements using laser-induced breakdown spectroscopy (LIBS). Food Res Int. 2017;94:72.
31. Babos DV, Barros AI, Nobrega JA, Pereira-Filho ER. Calibration strategies to overcome matrix effects in laser-induced breakdown spectroscopy: direct calcium and phosphorus determination in solid mineral supplements. Spectrochim Acta B. 2019;155:90.
32. Millar S, Gottlieb C, Günther T, Sankat N, Wilsch G, Kruschwitz S. Chlorine determination in cement-bound materials with laser-induced breakdown spectroscopy (LIBS)—a review and validation. Spectrochim Acta B. 2018;147:1.

33. Vieira AL, Silva TV, de Sousa FSI, Senesi GS, Júnior DS, Ferreira EC, Neto JAG. Determinations of phosphorus in fertilizers by spark discharge-assisted laser-induced breakdown spectroscopy. Microchem J. 2018;139:322.
34. Gomes MS, de Carvalho GGA, Santos D, Krug FJ. A novel strategy for preparing calibration standards for the analysis of plant materials by laser-induced breakdown spectroscopy: a case study with pellets of sugar cane leaves. Spectrochim Acta B. 2013;86:137.
35. Papai R, Sato RH, Nunes LC, Krug FJ, Gaubeur I. Melted paraffin wax as an innovative liquid and solid extractant for elemental analysis by laser-induced breakdown spectroscopy. Anal Chem. 2017;89:2807.
36. Andrade DF, Sperança MA, Pereira-Filho ER. Different sample preparation methods for the analysis of suspension fertilizers combining LIBS and liquid-to-solid matrix conversion: determination of essential and toxic elements. Anal Methods. 2017;9:5156.
37. Andrade DF, Guedes WN, Pereira FMV. Detection of chemical elements related to impurities leached from raw sugarcane: use of laser-induced breakdown spectroscopy (LIBS) and chemometrics. Microchem J. 2018;137:443.
38. Silvestre DM, Barbosa FM, Aguiar BT, Leme FO, Nomura CS. Feasibility study of calibration strategy for direct quantitative measurement of K and Mg in plant material by laser-induced breakdown spectrometry. Anal Chem Res. 2015;5:28.
39. Zhu Z, Li J, Guo Y, Cheng X, Tang Y, Guo L, Li X, Lu Y, Zeng X. Accuracy improvement of boron by molecular emission with a genetic algorithm and partial least squares regression model in laser-induced breakdown spectroscopy. J Anal At Spectrom. 2018;33:205.
40. Sweetapple MT, Tassios S. Laser-induced breakdown spectroscopy (LIBS) as a tool for in situ mapping and textural interpretation of lithium in pegmatite minerals. Am Mineral. 2015;100:2141.
41. Leme FO, Silvestre DM, Nascimento AN, Nomura CS. Feasibility of using laser induced breakdown spectroscopy for quantitative measurement of calcium, magnesium, potassium and sodium in meat. J Anal At Spectrom. 2018;33:1322.
42. de Carvalho GGA, Nunes LC, de Souza PF, Krug FJ, Alegre TC, Santos D Jr. Evaluation of laser induced breakdown spectrometry for the determination of macro and micronutrients in pharmaceutical tablets. J Anal At Spectrom. 2010;25:803.
43. Gu W, Song W, Yan G, Ye Q, Li Z, Afgan MS, Liu J, Song Y, Hou Z, Wang Z, Li Z. A data preprocessing method based on matrix matching for coal analysis by laser-induced breakdown spectroscopy. Spectrochim Acta B. 2021;180:106212.
44. Barnett WB, Fassel VA, Kniseley RN. Theoretical principles of internal standardization in analytical emission spectroscopy. Spectrochim Acta B. 1968;23:643.
45. Sperança MA, Pomares-Alfonso MS, Pereira-Filho ER. Analysis of Cuban nickeliferous minerals by laser-induced breakdown spectroscopy (LIBS): non-conventional sample preparation of powder samples. Anal Methods. 2018;10:533.
46. Zachariadis GA, Vogiatzis C. An overview of the use of yttrium for internal standardization in inductively coupled plasma–atomic emission spectrometry. Appl Spectrosc Rev. 2010;45:220.
47. Guezenoc J, Gallet-Budynek A, Bousquet B. Critical review and advices on spectral-based normalization methods for LIBS quantitative analysis. Spectrochim Acta B. 2019;160:105688.
48. Šindelářová A, Pořízka P, Modlitbová P, Vrlíková L, Kiss K, Kaška M, Prochazka D, Vrábel J, Buchtová M, Kaiser J. Methodology for the implementation of internal standard to laser-induced breakdown spectroscopy analysis of soft tissues. Sensors. 2021;21:900.
49. Juvé V, Portelli R, Boueri M, Baudelet M, Yu J. Space-resolved analysis of trace elements in fresh vegetables using ultraviolet nanosecond laser-induced breakdown spectroscopy. Spectrochim Acta B. 2008;63:1047.
50. Castro JP, Pereira-Filho ER. Twelve different types of data normalization for the proposition of classification, univariate and multivariate regression models for the direct analyses of alloys by laser-induced breakdown spectroscopy (LIBS). J Anal At Spectrom. 2016;31:2005.

51. Wu C, Sun DX, Su MG, Yin YP, Han WW, Lu QF, Dong CZ. Quantitative analysis of Pb in soil samples by laser-induced breakdown spectroscopy with a simplified standard addition method. J Anal At Spectrom. 2019;34:1478.
52. Zhu C, Lv J, Liu K, Li Q, Tang Z, Zhou R, Zhang W, Chen J, Liu K, Li X, Zeng X. Fast detection of harmful trace elements in glycyrrhiza using standard addition and internal standard method—laser-induced breakdown spectroscopy (SAIS-LIBS). Microchem J. 2021;168:106408.
53. Yi RX, Guo LB, Zou XH, Li JM, Hao ZQ, Yang XY, Li XY, Zeng XY, Lu YF. Background removal in soil analysis using laser- induced breakdown spectroscopy combined with standard addition method. Opt Express. 2016;24:2607.
54. Haider AFMY, Khan ZH. Determination of Ca content of coral skeleton by analyte additive method using the LIBS technique. Opt Laser Technol. 2012;44:1654.
55. Zivkovic S, Savovic J, Kuzmanovic M, Petrovic J, Momcilovic M. Alternative analytical method for direct determination of Mn and Ba in peppermint tea based on laser induced breakdown spectroscopy. Microchem J. 2018;137:410.
56. Bader MA. Systematic approach to standard addition methods in instrumental analysis. J Chem Educ. 1980;57:703.
57. Bilge G, Boyaci IH, Eseller KE, Tamer U, Cakir S. Analysis of bakery products by laser-induced breakdown spectroscopy. Food Chem. 2015;181:186.
58. Castro JP, Babos DV, Pereira-Filho ER. Calibration strategies for the direct determination of rare earth elements in hard disk magnets using laser-induced breakdown spectroscopy. Talanta. 2020;208:120443.
59. Virgilio A, Gonçalves DA, McSweeney T, Gomes Neto JA, Nóbrega JA, Donati GL. Multi-energy calibration applied to atomic spectrometry. Anal Chim Acta. 2017;982:31.
60. Babos DV, Virgilio A, Costa VC, Donati GL, Pereira-Filho ER. Multi-energy calibration (MEC) applied to laser-induced breakdown spectroscopy (LIBS). J Anal At Spectrom. 2018;33:1753.
61. Augusto AS, Castro JP, Sperança MA, Pereira-Filho EP. Combination of multi-energy calibration (MEC) and laser-induced breakdown spectroscopy (LIBS) for dietary supplements analysis and determination of Ca, Mg and K. J Braz Chem Soc. 2019;30:804.
62. Fortunato FM, Catelani TA, Pomares-Alfonso MS, Pereira-Filho ER. Application of multi-energy calibration for determination of chromium and nickel in nickeliferous ores by laser-induced breakdown spectroscopy. Anal Sci. 2019;35:165.
63. Carvalho AAC, Cozer LA, Luz MS, Nunes LC, Rocha FRP, Nomura CS. Multi-energy calibration and sample fusion as alternatives for quantitative analysis of high silicon content samples by laser-induced breakdown spectrometry. J Anal At Spectrom. 2019;34:1701.
64. Andrade DF, Fortunato FM, Pereira-Filho ER. Calibration strategies for determination of the in content in discarded liquid crystal displays (LCD) from mobile phones using laser-induced breakdown spectroscopy (LIBS). Anal Chim Acta. 2019;1061:42.
65. Li X, Zhao T, Zhong Q, Nie S, Xiao H, Zhao S, Huang W, Fan Z. Iterative multi-energy calibration and its application in online alloy smelting process monitoring using laser-induced breakdown spectroscopy. J Anal At Spectrom. 2020;35:2171.
66. Hao ZQ, Liu L, Zhou R, Ma YW, Li XY, Guo LB, Lu YF, Zeng XY. One-point and multi-line calibration method in laser-induced breakdown spectroscopy. Opt Express. 2018;26:22926.
67. Gamela RR, Costa VC, Babos DV, Araújo AS, Pereira-Filho ER. Direct determination of Ca, K, and Mg in cocoa beans by laser-induced breakdown spectroscopy (LIBS): evaluation of three univariate calibration strategies for matrix matching. Food Anal Methods. 2020;13:1017.
68. Vieira AL, Ferreira EC, Júnior DS, Senesi GS, Neto JAG. Spark discharge-libs: evaluation of one-point and multi-voltage calibration for p and al determination. At Spectrosc. 2021;42:18.
69. Yuan R, Tang Y, Zhu Z, Hao Z, Li J, Yu H, Yu Y, Guo L, Zeng X, Lu Y. Accuracy improvement of quantitative analysis for major elements in laser-induced breakdown spectroscopy using single-sample calibration. Anal Chim Acta. 2019;1064:11.

70. Nunes LC, Rocha FRP, Krug FJ. Slope ratio calibration for analysis of plant leaves by laser-induced breakdown spectroscopy. J Anal At Spectrom. 2019;34:2314.
71. Costa VC, de Mello ML, Babos DV, Castro JP, Pereira-Filho ER. Calibration strategies for determination of Pb content in recycled polypropylene from car batteries using laser-induced breakdown spectroscopy (LIBS). Microchem J. 2020;159:105558.
72. Krutchkoff RG. Classical and inverse regression methods of calibration. Technometrics. 1967;9:425.
73. Duponchel L, Bousquet B, Pelascini F, Motto-Ros V. Should we prefer inverse models in quantitative LIBS analysis? J Anal At Spectrom. 2020;35:794.
74. de Carvalho GGA, Santos D, Nunes LC, Gomes MS, Leme F d O, Krug FJ. Effects of laser focusing and fluence on the analysis of pellets of plant materials by laser-induced breakdown spectroscopy. Spectrochim Acta B. 2012;74–75:162.
75. Machado RC, Babos DV, Andrade DF, Pereira-Filho ER. A novel strategy for direct elemental determination using laser-induced breakdown spectroscopy: fluence calibration. J Anal At Spectrom. 2021;36:2132.
76. Zhang T, Tang H, Li H. Chemometrics in laser-induced breakdown spectroscopy. J Chemometr. 2018;32:1.
77. Geladi P, Kowalski BR. Partial least-squares regression: a tutorial. Anal Chim Acta. 1986;185:1.
78. Brereton RG. Introduction to multivariate calibration in analytical chemistry. Analyst. 2000;125:2125.
79. Ayyalasomayajula KK, Yu-Yueh F, Singh JP, McIntyre DL, Jain J. Application of laser-induced breakdown spectroscopy for total carbon quantification in soil samples. Appl Optics. 2012;51:149.
80. Wang J, Xue S, Zheng P, Chen Y, Peng R. Determination of lead and copper in Ligusticum wallichii by laser-induced breakdown spectroscopy. Anal Lett. 2017;50:2000.
81. Sperança MA, Andrade DF, Castro JP, Pereira-Filho ER. Univariate and multivariate calibration strategies in combination with laser-induced breakdown spectroscopy (LIBS) to determine Ti on sunscreen: a different sample preparation procedure. Opt Laser Technol. 2019;109:648.
82. Ayyalasomayajula KK, McIntyre DL, Jain J, Singh JP, Yu-Yueh F. Determination of elemental impurities in plastic calibration standards using laser-induced breakdown spectroscopy. Appl Optics. 2012;51:B1.
83. Wen S, Jiang-tao L, Cui-ping L, Chun-hou Z. Quantitative analysis of P in compound fertilizer by laser-induced breakdown spectroscopy coupled with linear multivariate calibration. Spectrosc Spect Anal. 2019;39:1958.
84. Yaroshchyk P, Death DL, Spencer SJ. Comparison of principal components regression, partial least squares regression, multi-block partial least squares regression, and serial partial least squares regression algorithms for the analysis of Fe in iron ore using LIBS. J Anal At Spectrom. 2012;27:92.
85. Zaytsev SM, Popov AM, Chernykh EV, Voronina RD, Zorov NB, Labutin TA. Comparison of single- and multivariate calibration for determination of Si, Mn, Cr and Ni in high-alloyed stainless steels by laser-induced breakdown spectrometry. J Anal At Spectrom. 2014;29:1417.
86. Devangad P, Unnikrishnan VK, Tamboli MM, Shameem KMM, Nayak R, Choudhari KS, Santhosh C. Quantification of Mn in glass matrices using laser induced breakdown spectroscopy (LIBS) combined with chemometric approaches. Anal Methods. 2016;8:7177.
87. Takahashi T, Thornton B, Sato T, Ohki T, Ohki K, Sakka T. Temperature based segmentation for spectral data of laser-induced plasmas for quantitative compositional analysis of brass alloys submerged in water. Spectrochim Acta B. 2016;124:87.
88. Hernández-García R, Villanueva-Tagle ME, Calderón-Piñar F, Durruthy-Rodríguez MD, Aquino FWB, Pereira-Filho ER, Pomares-Alfonso MS. Quantitative analysis of lead zirconate titanate (PZT) ceramics by laser-induced breakdown spectroscopy (LIBS) in combination with multivariate calibration. Microchem J. 2017;130:21.

89. Costa VC, Pereira FMV. Laser-induced breakdown spectroscopy applied to the rapid identification of different types of polyethylene used for toy manufacturing. J Chemometr. 2020;34:1.
90. Castro JP, Pereira-Filho ER, Bro R. Laser-induced breakdown spectroscopy (LIBS) spectra interpretation and characterization using parallel factor analysis (PARAFAC): a new procedure for data and spectral interference processing fostering the waste electrical and electronic equipment (WEEE) recycling process. J Anal At Spectrom. 2020;35:1115.
91. Andrade DF, Pereira-Filho ER, Konieczynski P. Comparison of ICP OES and LIBS analysis of medicinal herbs rich in flavonoids from Eastern Europe. J Braz Chem Soc. 2017;28:838.
92. Goueguel CL, Soumare A, Nault C, Nault J. Direct determination of soil texture using laser-induced breakdown spectroscopy and multivariate linear regressions. J Anal At Spectrom. 2019;34:1588.
93. Costa VC, Aquino FWB, Paranhos CM, Pereira-Filho ER. Use of laser-induced breakdown spectroscopy for the determination of polycarbonate (PC) and acrylonitrile-butadiene-styrene (ABS) concentrations in PC/ABS plastics from e-waste. Waste Manag. 2017;70:121.
94. Ding Y, Xia G, Ji H, Xiong X. Accurate quantitative determination of heavy metals in oily soil by laser induced breakdown spectroscopy (LIBS) combined with interval partial least squares (IPLS). Anal Methods. 2019;11:3657.
95. Zhang T-L, Wu S, Tang H-S, Wang K, Duan Y-X, Li H. Progress of chemometrics in laser-induced breakdown spectroscopy analysis. Chin J Anal Chem. 2015;43:939.
96. Li L-N, Liu X-F, Yang F, Xu W-M, Wang J-Y, Shu R. A review of artificial neural network based chemometrics applied in laser-induced breakdown spectroscopy analysis. Spectrochim Acta B. 2021;180:106183.
97. Ferreira EC, Milori DMBP, Ferreira EJ, Da Silva RM, Martin-Neto L. Artificial neural network for Cu quantitative determination in soil using a portable laser induced breakdown spectroscopy system. Spectrochim Acta B. 2008;63:1216.
98. D'Andrea E, Pagnotta S, Grifoni E, Legnaioli S, Lorenzetti G, Palleschi V, Lazzerini B. A hybrid calibration-free/artificial neural networks approach to the quantitative analysis of LIBS spectra. Appl Phys B Lasers Opt. 2015;118:353.
99. El Haddad J, Bruyère D, Ismaël A, Gallou G, Laperche V, Michel K, Canioni L, Bousquet B. Application of a series of artificial neural networks to on-site quantitative analysis of lead into real soil samples by laser induced breakdown spectroscopy. Spectrochim Acta B. 2014;97:57.
100. Lu C, Wang B, Jiang X, Zhang J, Niu K, Yuan Y. Detection of K in soil using time-resolved laser-induced breakdown spectroscopy based on convolutional neural networks. Plasma Sci Technol. 2018;21:034014.
101. D'Andrea E, Pagnotta S, Grifoni E, Lorenzetti G, Legnaioli S, Palleschi V, Lazzerini B. An artificial neural network approach to laser-induced breakdown spectroscopy quantitative analysis. Spectrochim Acta B. 2014;99:52.
102. Li K, Guo L, Li C, Li X, Shen M, Zheng Z, Yu Y, Hao R, Hao Z, Zeng Q, Lu Y, Zeng X. Analytical-performance improvement of laser-induced breakdown spectroscopy for steel using multi-spectral-line calibration with an artificial neural network. J Anal At Spectrom. 2015;30:1623.
103. Lorenzetti G, Legnaioli S, Grifoni E, Pagnotta S, Palleschi V. Laser-based continuous monitoring and resolution of steel grades in sequence casting machines. Spectrochim Acta B. 2015;112:1.
104. Inakollu P, Philip T, Rai AK, Yueh F-Y, Singh JP. A comparative study of laser induced breakdown spectroscopy analysis for element concentrations in aluminum alloy using artificial neural networks and calibration methods. Spectrochim Acta B. 2009;64:99.
105. Bhatt B, Angeyo KH, Dehayem-Kamadjeu A. LIBS development methodology for forensic nuclear materials analysis. Anal Methods. 2018;10:791.
106. Lu Z, Mo J, Yao S, Zhao J, Lu J. Rapid determination of the gross calorific value of coal using laser-induced breakdown spectroscopy coupled with artificial neural networks and genetic algorithm. Energy Fuel. 2017;31:3849.

107. Wang J, Shi M, Zheng P, Xue S, Peng R. Quantitative analysis of Ca, Mg, and K in the roots of Angelica pubescens f. biserrata by laser-induced breakdown spectroscopy combined with artificial neural networks. J Appl Spectrosc. 2018;85:190.
108. Hu Y, Li Z, Lü T. Determination of elemental concentration in geological samples using nanosecond laser-induced breakdown spectroscopy. J Anal At Spectrom. 2017;32:2263.
109. Galbács G, Gornushkin IB, Smith BW, Winefordner JD. Semi-quantitative analysis of binary alloys using laser-induced breakdown spectroscopy and a new calibration approach based on linear correlation. Spectrochim Acta B. 2001;56:1159.
110. Galbács G, Jedlinszki N, Cseh G, Galbács Z, Túri L. Accurate quantitative analysis of gold alloys using multi-pulse laser induced breakdown spectroscopy and a correlation-based calibration method. Spectrochim Acta B. 2008;63:591.
111. Galbács G, Gornushkin IB, Winefordner JD. Generalization of a new calibration method based on linear correlation. Talanta. 2004;63:351.
112. Meng T, Jing X, Yan Z, Pedrycz W. A survey on machine learning for data fusion. Inf Fusion. 2020;57:115.
113. Brereton RG, Jansen J, Lopes J, Marini F, Pomerantsev A, Rodionova O, Roger JM, Walczak B, Tauler R. Chemometrics in analytical chemistry-part I: history, experimental design and data analysis tools. Anal Bioanal Chem. 2017;409:5891.
114. Geladi P. Chemometrics in spectroscopy. Part 1. Classical chemometrics. Spectrochim Acta B. 2003;58:767.
115. Lahat D, Adali T, Jutten C. Multimodal data fusion: an overview of methods, challenges, and prospects. Proc IEEE. 2015;103:1449.
116. Borràs E, Ferré J, Boqué R, Mestres M, Aceña L, Busto O. Data fusion methodologies for food and beverage authentication and quality assessment—a review. Anal Chim Acta. 2015;891:1.
117. Guedes WN, Pereira FMV. Classifying impurity ranges in raw sugarcane using laser-induced breakdown spectroscopy (LIBS) and sum fusion across a tuning parameter window. Microchem J. 2018;143:331.
118. Szymańska E. Modern data science for analytical chemical data—a comprehensive review. Anal Chim Acta. 2018;1028:1.
119. Stefas D, Gyftokostas N, Kourelias P, Nanou E, Kokkinos V, Bouras C, Couris S. Discrimination of olive oils based on the olive cultivar origin by machine learning employing the fusion of emission and absorption spectroscopic data. Food Control. 2021;130:108318.
120. Gamela RR, Costa VC, Sperança MA, Pereira-Filho ER. Laser-induced breakdown spectroscopy (LIBS) and wavelength dispersive X-ray fluorescence (WDXRF) data fusion to predict the concentration of K, Mg and P in bean seed samples. Food Res Int. 2020;132:109037.
121. Gamela RR, Pereira-Filho ER, Pereira FMV. Minimal-invasive analytical method and data fusion: an alternative for determination of Cu, K, Sr, and Zn in cocoa beans. Food Anal Methods. 2021;14:545.
122. Andrade DF, Almeida E, Carvalho HWP, Pereira-Filho ER, Amarasiriwardena D. Chemical inspection and elemental analysis of electronic waste using data fusion—application of complementary spectroanalytical techniques. Talanta. 2021;225:122025.
123. Santos MC, Pereira FMV. Direct analysis of human hair before and after cosmetic modification using a recent data fusion method. J Braz Chem Soc. 2020;31:33.
124. de Oliveira DM, Fontes LM, Pasquini C. Comparing laser induced breakdown spectroscopy, near infrared spectroscopy, and their integration for simultaneous multi-elemental determination of micro- and macronutrients in vegetable samples. Anal Chim Acta. 2019;1062:28.
125. Xu D, Zhao R, Li S, Chen S, Jiang Q, Zhou L, Shi Z. Multi-sensor fusion for the determination of several soil properties in the Yangtze River Delta, China. Eur J Soil Sci. 2019;70:162.
126. Xu X, Du C, Ma F, Shen Y, Wu K, Liang D, Zhou J. Detection of soil organic matter from laser-induced breakdown spectroscopy (LIBS) and mid-infrared spectroscopy (FTIR-ATR) coupled with multivariate techniques. Geoderma. 2019;355:113905.

127. Manrique-Martinez JA, Lopez-Reyes G, Alvarez-Perez A, Bozic T, Veneranda M, Sanz-Arranz A, Saiz J, Medina-Garcia J, Rull-Perez F. Evaluation of multivariate analyses and data fusion between Raman and laser-induced breakdown spectroscopy in binary mixtures and its potential for solar system exploration. J Raman Spectrosc. 2020;51:1.
128. Araújo AS, Castro JP, Sperança MA, Andrade DF, Mello ML, Pereira-Filho ER. Multiway calibration strategies in laser-induced breakdown spectroscopy: a proposal. Anal Chem. 2021;93:6291.
129. Costa VC, Castro JP, Andrade DF, Victor Babos D, Garcia JA, Sperança MA, Catelani TA, Pereira-Filho ER. Laser-induced breakdown spectroscopy (LIBS) applications in the chemical analysis of waste electrical and electronic equipment (WEEE). TrAC Trends Anal Chem. 2018;108:65.
130. Elmasry G, Kamruzzaman M, Sun D-W, Allen P. Principles and applications of hyperspectral imaging in quality evaluation of agro-food products: a review. Crit Rev Food Sci Nutr. 2012;52:999.
131. Wu D, Sun D-W. Advanced applications of hyperspectral imaging technology for food quality and safety analysis and assessment: a review—part I: fundamentals. Innov Food Sci Emerg Technol. 2013;19:1.
132. Gamela RR, Sperança MA, Andrade DF, Pereira-Filho ER. Hyperspectral images: a qualitative approach to evaluate the chemical profile distribution of Ca, K, Mg, Na and P in edible seeds employing laser-induced breakdown spectroscopy. Anal Methods. 2019;11:5543.
133. Amigo JM, Babamoradi H, Elcoroaristizabal S. Hyperspectral image analysis. A tutorial. Anal Chim Acta. 2015;896:34.
134. Edelman GJ, Gaston E, van Leeuwen TG, Cullen PJ, Aalders MCG. Hyperspectral imaging for non-contact analysis of forensic traces. Forensic Sci Int. 2012;223:28.
135. Wu D, Meng L, Yang L, Wang J, Fu X, Du X, Li S, He Y, Huang L. Feasibility of laser-induced breakdown spectroscopy and hyperspectral imaging for rapid detection of thiophanate-methyl residue on mulberry fruit. Int J Mol Sci. 2019;20:1.
136. Garcia JA, da Silva JRA, Pereira-Filho ER. LIBS as an alternative method to control an industrial hydrometallurgical process for the recovery of Cu in waste from electro-electronic equipment (WEEE). Microchem J. 2021;164:106007.
137. Carter S, Clough R, Fisher A, Gibson B, Russell B. Atomic spectrometry update: review of advances in the analysis of metals, chemicals and materials. J Anal At Spectrom. 2021;36:2241.
138. Lazic V, Jovićević S. Laser induced breakdown spectroscopy inside liquids: processes and analytical aspects. Spectrochim Acta B. 2014;101:288.
139. Jantzi SC, Motto-Ros V, Trichard F, Markushin Y, Melikechi N, De Giacomo A. Sample treatment and preparation for laser-induced breakdown spectroscopy. Spectrochim Acta B. 2016;115:52.
140. Costa VC, Augusto AS, Castro JP, Machado RC, Andrade DF, Babos DV, Sperança MA, Gamela RR, Pereira-Filho ER. Laser induced-breakdown spectroscopy (LIBS): histórico, fundamentos, aplicações e potencialidades. Quim Nova. 2019;42:527.